Out-of-Plane Behavior of Dowel Type Precast Concrete Panel-to-Foundation Connections: Existing Connections

Hogan[1], L.S., Henry, R.S. [1], and Ingham, J. M. [1]

Abstract:

Precast concrete wall panels are a common structural system, particularly in low-rise industrial and commercial buildings. Such buildings can represent a large proportion of the building stock, yet the connections between precast concrete panels and other structural members have been found to perform poorly in past earthquakes. Fourteen panels were tested to investigate the out-of-plane performance of common precast panel to foundation dowel connections. Panel details included both dowel starter bars formed from conventional reinforcing steel, such has hooked bars, as well as starter bars connected to the panel with cast in threaded inserts. Panel and connection strengths were varied and panel details were subjected to both cyclic and monotonic loading. It was found that the conventional starter bars performed well due to additional strengthening in the joint region, while the threaded insert panels degraded in strength once flexural cracking propagated vertically in the joint behind the insert heads and separating the panel from the starter bars. In instances where connection details were found to provide inadequate behavior, alternative details were proposed and tested. These connection details and their performance are reported in a companion paper entitled: *Out-of-Plane Behavior of Dowel Type Precast Concrete Panel-to-Foundation Connections: Alternative Connections.*

1)   *Department of Civil and Environmental Engineering, University of Auckland, Auckland, New Zealand*
     lucas.hogan@aucklanduni.ac.nz, rs.henry@auckland.ac.nz, and j.ingham@auckland.ac.nz

1   INTRODUCTION

Precast concrete panels are a widely used construction form in low-rise industrial buildings. These buildings can represent a substantial portion of the building stock, and their post-earthquake functionality has important economic implications given their use as warehouse and distribution centers. Despite these buildings being typically designed for an elastic or nominally ductile seismic response, they have been found to perform poorly in earthquakes, often due to failure of connections (Hamburger et al. 1988, Adham et al. 1996). While, earthquake reconnaissance following the 2010/2011 Canterbury earthquake sequence in New Zealand found that overall, precast and tilt-up concrete buildings performed adequately (Henry and Ingham 2011), vulnerabilities were identified in the out-of-plane response of dowel type panel-to-foundation connections for panels with a single layer of vertical reinforcing, particularly for panels that utilized threaded inserts embedded in the panels to connect starter bars to the foundation (SESOC 2013). An example of a dowel type panel-to-foundation connection is shown in Figure 1. The use of threaded inserts has become popular in New Zealand for precast panel construction because the starter bars can be screwed into the panels after they were erected and thus avoided the need to bend bars for transport and storage thus reducing labor and time on site prior to pouring of the foundation (Beattie 2007). Because of the low out-of-plane strength of the panels, the demands on the starter bar reinforcement are typically below yield, and the pullout strength of the inserts often governs the

2

43   design of the foundation connection. As such, when the panel is loaded with a joint-opening

44   moment, the concrete behind the insert head is required to act in tension to complete the primary

45   load path (Figure 2), and when subjected to large moments, a vertical crack in the panel could

46   develop as the concrete behind the insert head ruptures causing a significant loss in strength and

47   stiffness. The limited testing on this type of connection performed by Ma (2000) showed that

48   while no vertical cracking in the panel joint region was observed when using an embedment depth

49   to panel thickness ratio of 0.87, the connection could not sustain the nominal moment capacity of

50   the panel in the joint opening direction. Current practice typically uses a shallower embedment

51   depth to panel thickness ratio of approximately 0.67, and it is expected that this shallower

52   embedment could result in brittle joint failure. To investigate the strength and deformation

53   capacity of typical threaded insert connections, a series precast panel to foundation connections of

54   different nominal panel and joint connection strengths were subjected to out-of-plane loading.

55   Performance of threaded insert connections was compared to connections without inserts that

56   utilized starter bars with conventional hooked bar anchorage, as these are also a common

57   connection type with potentially similar vulnerabilities as the threaded insert connections. Finally,

58   where connection details were found to provide inadequate behavior, alternative details were

59   proposed and tested. These details and their performance are reported in a companion paper

60   entitled: *Out-of-Plane Behavior of Dowel Type Precast Concrete Panel-to-Foundation Connections:*

61   *Alternative Connections.*

62
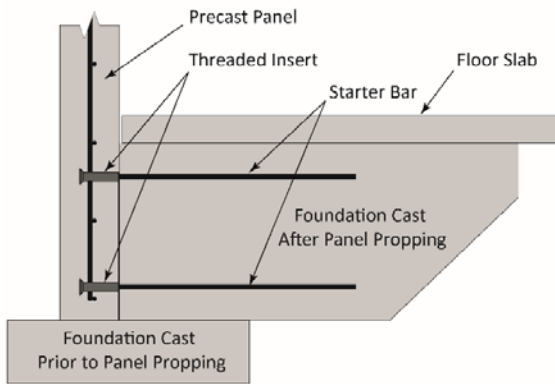
Figure 1: Schematic representation of a dowel type precast panel to foundation connection utilizing threaded inserts.
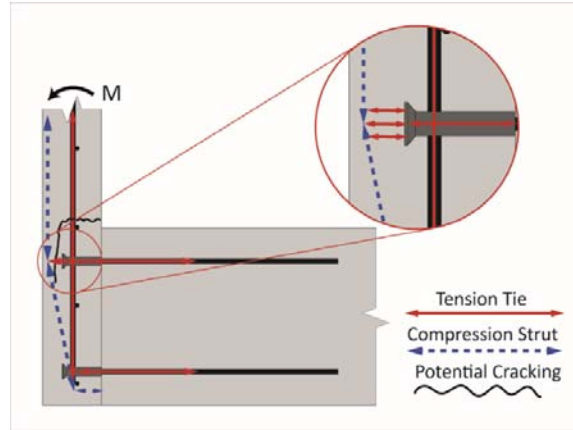

Figure 2: Strut and tie representation of load path for panel to foundation connection using threaded inserts with a shallow embedment depth

63   **2   TEST DESCRIPTION**

64   **2.1   Prototype Development**

65   Test panel detailing was determined from a survey of over 4700 panels produced by precast

66   companies throughout New Zealand (Seifi et al. 2016).   From this survey it was determined that

67   panel dimensions in low-rise industrial buildings were typically 10 m tall, between 2 to 3 m wide,

68   and 150 mm thick.   These panels typically only support their self-weight as gravity load and are

69   incorporated in buildings with light flexible diaphragms constructed of steel decking and wall

70   lengths that are between 10 to 60 m.   This low level of seismic demand and the panel geometry

71   mean that often only minimum reinforcement is required, and this reinforcement is typically either

4

72 grade 500 (f_y = 500 MPa) 12 mm or 16 mm diameter bars (i.e. HD12 and HD16) in a single layer

73 (or curtain).

74 Due to the difficulty in testing full scale panels, a prototype panel was developed based upon a 10 m

75 tall panel with fixed base and pinned top boundary conditions subjected to a uniform distributed

76 load representing the inertial face loading of the panel in the out-of-plane direction, as shown in

77 Figure 3.   The moment and shear demands on the bottom 2.5 m height of the panel were

78 approximately equivalent to that of a point load at the top of a 2.5 m cantilever panel.   As the

79 out-of-plane response was being investigated, only a unit width of panel was tested to allow for all

80 requisite panels to fit on the test site.   From these considerations the test panels were constructed to

81 be 2.5 m tall and were cast into a self-reacting test set up, as shown in Figure 4.   Panels were

82 erected on top of a 200 mm tall strip foundation and starter bars were installed or bent into place as

83 required, after which the foundation beam was constructed in-situ.   Load was applied to the panel

84 top by a hydraulic jack reacting against a steel column that was bolted to the foundation opposite

85 the panel.   Apart of the panel self-weight, no additional axial load was applied as axial load ratios

86 of these panels are typically low (~0.4% $A_g f_c$').
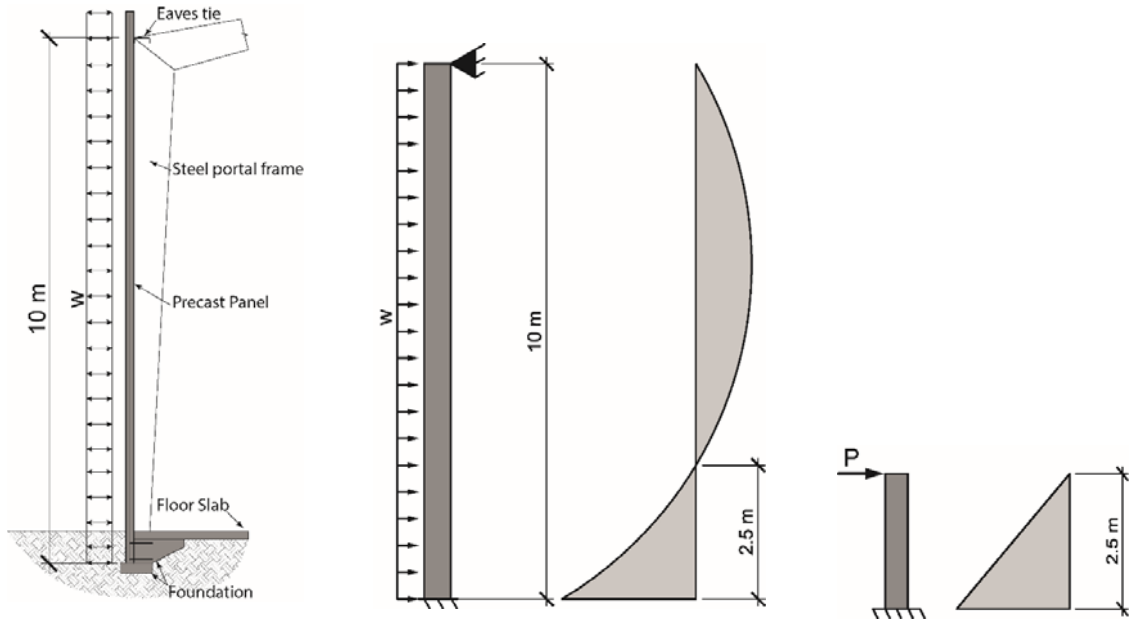
(a) Schematic section of 10 m tall panel subjected to face loading

(b) Boundary condition representation and moment distribution of panel

(c) Cantilever loading approximation for test set up

Figure 3: Prototype panel development based upon moment distribution

87
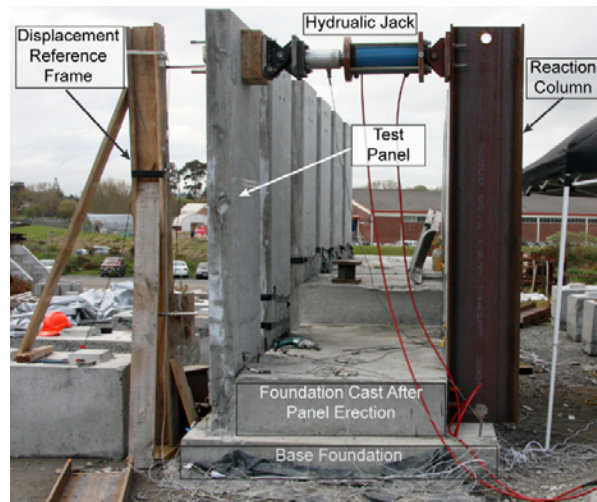
Figure 4: Panel test set up

88 2.2 Test Panel Description

89 Based upon the panel survey by Seifi et al. (2016), fourteen panels were constructed using nine

90 different reinforcement configurations, which are summarized in Table 1. All panels were

91 2500 mm tall and 150 mm thick with a single layer of reinforcing in the center of the panel.

92 Twelve of the fourteen panels were 900 mm wide with the other two panels being 1062 mm wide.

93 Panel strength, foundation height and connection type were varied to investigate the behavior of

94 typical panels as was determined by the panel survey. The panel to foundation connections of

95 these panels fall into three main categories: a bolted through connection that served as a control

96 specimen, conventional starter bars, and starter bars using threaded inserts.

97 The control specimen (BLT12-C0) utilized starter bars that extended all the way through the panel

98 and were bolted to steel rectangular hollow sections on the back face of the panel as is shown in

99 Figure 5. While this connection type is not used in practice, it was tested as a control case because

100 the extension of the starter bars through the panel provided a tension tie into the compression zone

101 of the panel during joint-opening moment. As such, the load path described in Figure 2 no longer

102 had to rely upon concrete acting in tension and thus avoided the brittle failure mechanism caused by

103 vertical cracking of the panel in the joint region. The panel had HD 12 (diameter = 12 mm, f_y =

104 500 MPa) vertical reinforcing at 270 mm spacing and HD 10 (diameter = 10 mm, f_y = 500 MPa)

105 horizontal reinforcing at 200 mm spacing. The eight starter bars were aligned with the vertical

7

106   reinforcing and were distributed in two rows 85 mm from both the top and bottom of the 450 mm

107   tall foundation (Figure 5b).

108   Two versions of conventionally reinforced starter bar connections were tested to compare the

109   performance of conventionally anchored starter bars to those anchored with threaded inserts.   The

110   first conventional starter bar panel utilized two layers of "L" type starter bars (Panel DL12-C50)

111   and the other panel used "U" bars (Panel U12-C50), also commonly referred to as "hairpin" starter

112   bars.   Both panels had the same HD 12 vertical reinforcing at 270 mm spacing and HD 10

113   horizontal reinforcing at 200 mm spacing as the bolted through control panel as well as a 450 mm

114   tall foundation.   Panel DL12-C50 utilized two rows of four D12 (diameter = 12 mm, f_y = 300 MPa)

115   hooked bars with 600 mm returns aligned with the vertical reinforcement as starter bars (Figure 6a),

116   while Panel U12-C50 utilized four D12 bars bent in a "U" shape as starter bars (Figure 6b).   Both

117   conventional starter bars utilized D12 bars at the bends of the hooks or U bars to develop the bar in

118   the panel.   Grade 300 reinforcing (f_y = 300 MPa) was used for the conventional starter bars to align

119   with typical detailing practice and allow for the bars to be bent up flush to the panel face for storage

120   and transport and re-straightened for panel erection.   Starter bars in Panels DL12-C50 and

121   U12-C50 were bent and re-straightened to simulate this construction practice.

122   The threaded insert connections were tested in different configurations of panel strength, insert

123   embedment depth, and insert spacing.   Different panel and foundation strengths were investigated

124 by testing panels with either HD12 vertical reinforcing at 270 mm centers or HD16 (diameter = 16

125 mm, f_y = 500 MPa) at 270 mm centers.   The starter bars used for the threaded insert panels were a

126 propriety reinforcement with the same mechanical properties to the HD bars, but with deformations

127 that allowed it to be threaded into the cast-in-inserts, and are denoted as RB and the diameter of the

128 reinforcing (e.g. RB12 for 12 mm diameter bars) in this paper.   Starter bars had the same diameter

129 as the vertical reinforcing (e.g. 12 mm diameter starter bars for panels with HD12 vertical

130 reinforcing).   Panels that utilized 12 mm vertical reinforcing and starter bars are denoted with the

131 prefix TI12 in Table 1 and Figure 7, and those that utilized 16 mm vertical reinforcing and starter

132 bars have a prefix TI16 in Table 1 and Figure 8.   All 12 mm insert panels except Panel

133 TI12-C50-FC and TI12-C50-FC-M had 350 mm tall foundations which are common for panels of

134 these strengths while, the 16 mm inserts were cast into a 710 mm tall foundations to investigate the

135 behavior of deeper foundations which are found in stronger panels that are likely to attract larger

136 overturning forces (Seifi et al. 2016).

137 The effect of insert embedment depth was examined by testing panels of using two different insert

138 sizes and construction methods that varied the embedment depths.   The base case for both the

139 12 mm inserts and 16 mm inserts was such that the insert was installed flush with the panel face and

140 had an embedment length equal to that of the insert length.   These panels are Panel TI12-C50 and

141 TI16-C32 for the 12 mm starter bar and 16 mm starter bar panels respectively, where C50 and C32

142 refers to the clear cover (50 mm or 32mm) behind the insert head to the back of the 150 mm thick

143 panel.   As an alternative to casting the insert flush with the panel face, Panels TI12-C42 and

144 Panels TI16-C24 utilized an 8 mm thick plastic nail plate, which is commonly used to mount

145 threaded inserts to formwork and resulted in a reduced cover of 42 mm and 24 mm, respectively.

146 This configuration was investigated to determine whether or not the additional embedment depth

147 improved the performance as well as to inspect the effect of filling the nail plate void during

148 foundation pouring has on the stiffness of the connection and slip of the starter bars in the insert.

149 The configuration and spacing of the inserts in the foundation was also investigated to determine

150 the consequence of overlapping failure cones, initiated during insert pullout, on the behavior of the

151 connection.   All inserts had a minimum horizontal spacing of 300 mm and consisted of two rows

152 of three inserts for all insert panels, and as such the inserts were not aligned with the vertical

153 reinforcing (Figure 7c and Figure 8c).   Such detailing is common in practice as inserts are often

154 puddled into fresh concrete and such spacing allows the inserts to be installed without conflicting

155 with the vertical reinforcement.   For both the 12 mm and 16 mm inserts, two panels were

156 constructed that allowed for the inserts to develop the full theoretical failure cone without failure

157 cones of adjacent inserts overlapping based on the design equations present in the New Zealand

158 Concrete Structures Standard, NZS 3101:2006 (Standards New Zealand 2006), which are the

159 equations as those in Appendix D of ACI 318-08 (ACI 2008).   These panels had the inserts

160   installed flush with the panel face and are denoted as TI12-C50-FC and TI16-C32-FC. Panel

161   TI12-C50-FC was cast with a 710 mm foundation and Panel TI16-C32-FC was cast with a slightly

162   wider panel to accommodate these failure cones.

Table 1: Test panel connection details

Panel Name	Connection Type	Connection Description	Vert Reinf	Foundation Height (mm)	Cover behind insert (mm)	Starter bars per layer
BLT12-C0	Control	Bolted through	HD12	450	N/A	4
DL12-C50	Conventional Starter Bar	Double L – D12	HD12	450	50	4
U12-C50	Conventional Starter Bar	U Bar – D12	HD12	450	50	4
TI12-C50	Threaded Insert	TI12	HD12	350	50	3
TI12-C42	Threaded Insert	TI12 + Nail plate	HD12	350	42	3
TI12-C42-M	Threaded Insert	TI12 + Nail plate	HD12	350	42	3
TI12-C50-FC	Threaded Insert	TI12 Full Cone	HD12	710	50	3
TI12-C50-FC-M	Threaded Insert	TI12 Full Cone	HD12	710	50	3
TI16-C32	Threaded Insert	TI16	HD16	710	32	3
TI16-C32-M	Threaded Insert	TI16	HD16	710	32	3
TI16-C24	Threaded Insert	TI16 + Nail plate	HD16	710	24	3
TI16-C24-M	Threaded Insert	TI16 + Nail plate	HD16	710	24	3
TI16-C32-FC	Threaded Insert	TI16 Full Cone	HD16	710	32	3
TI16-C32-FC-M	Threaded Insert	TI16 Full Cone	HD16	710	32	3

[a] TI = Threaded Insert; number following is diameter of starter bar

[b] M in panel name denotes monotonic loading

[c] All vertical reinforcing spaced at 270 mm

163
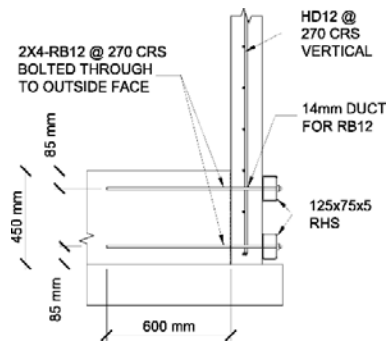
(a) Panel BLT12-C0
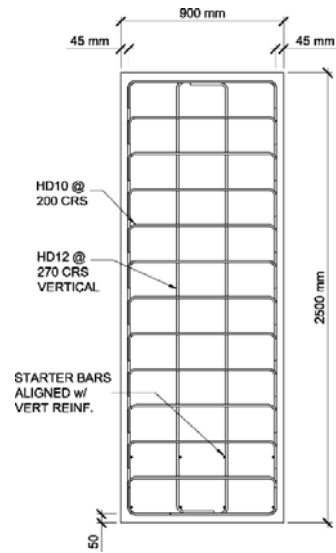
(b) Typical Panel Reinforcing

Figure 5: Details of bolted through foundation connection tested and panel reinforcing

164
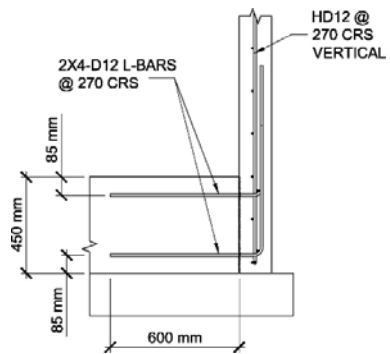
(a) Panel DL12-C50
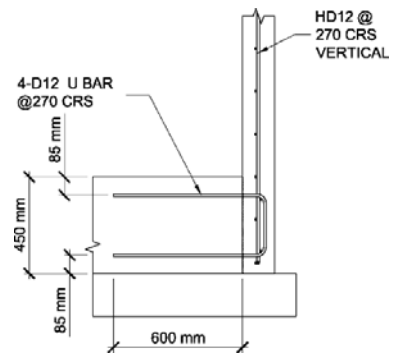
(b) Panel U12-C50

Figure 6: Details of conventional starter bar foundation connections tested

165
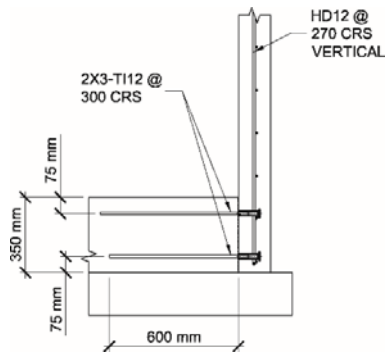
(a) Panel TI12-C50
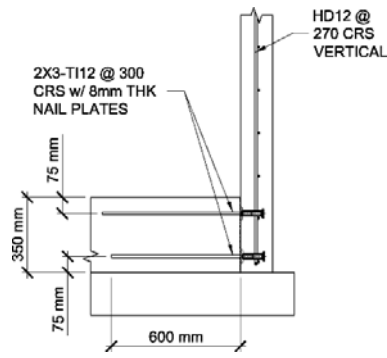
(b) Panel TI12-C42
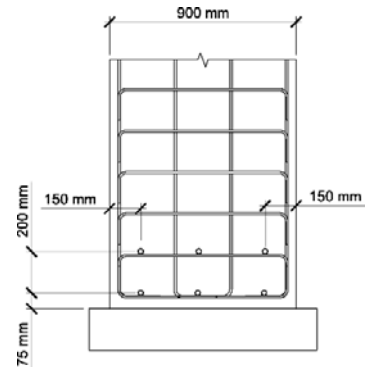
(c) Insert Spacing for Panels
TI12-C50 & TI12-C42
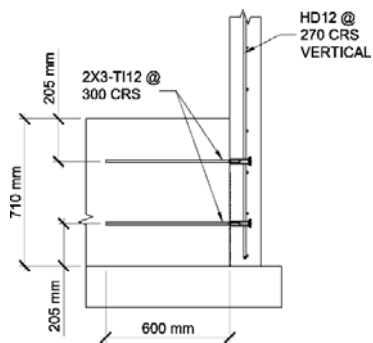
(d) Panel TI12-C50FC
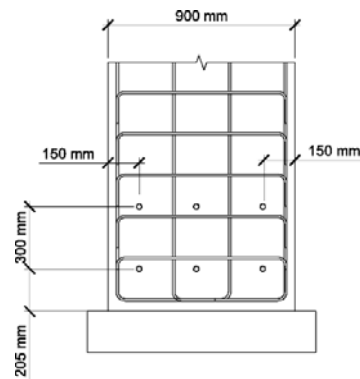
(e) Insert Spacing for Panel TI12-C50FC

Figure 7: Details of 12 mm threaded insert foundation connections tested

166

167
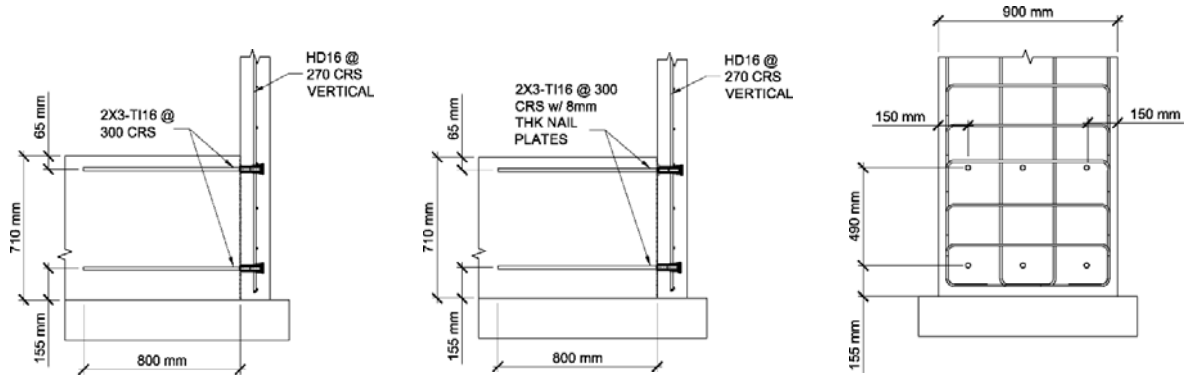
(a) Panel TI16-C32   (b) Panel TI16-C24   (c) Insert Spacing for Panels TI16-C32 & TI16-C24
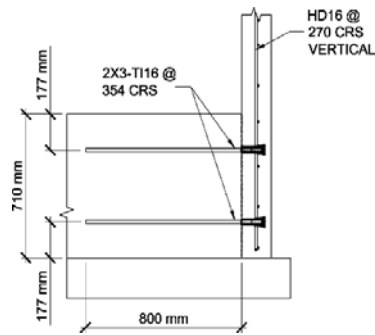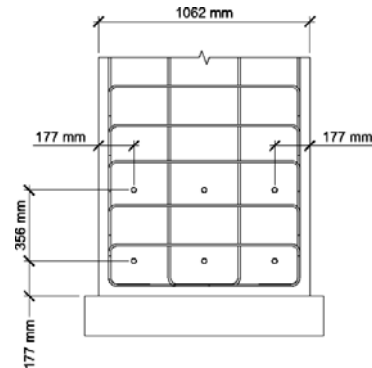
(d) Panel TI16-C32FC   (e) Insert Spacing for Panel TI16-C32FC

Figure 8: Details of 16 mm threaded insert foundation connections tested

168

2.3   Testing Protocol

169

170   Nine of the fourteen panels tested were subjected to cyclic loading using a loading protocol that was

171   developed based on recommendations by ACI (2007, 2013) which is shown in Figure 9. The

172   protocol consisted of one load controlled cycle at 60% of theoretical panel yield followed by three

173   cycles of displacement controlled cycles at increasing drift levels. Target drift levels were 0.5%,

174   1.0%, 1.5%, 2.0%, 3.0%, 4.5% and 6.25% drift calculated using the height of the 2.5 m cantilever

175   panel.

176   Five panels were subjected to monotonic loading to investigate the load path vulnerability in the

177   joint-opening direction directly and determine if the failure mechanism was sensitive to cyclic

178   loading.   These panels were constructed using the same reinforcing and connection details as

179   panels subjected to cyclic loading but are denoted with an "M" in Table 1.
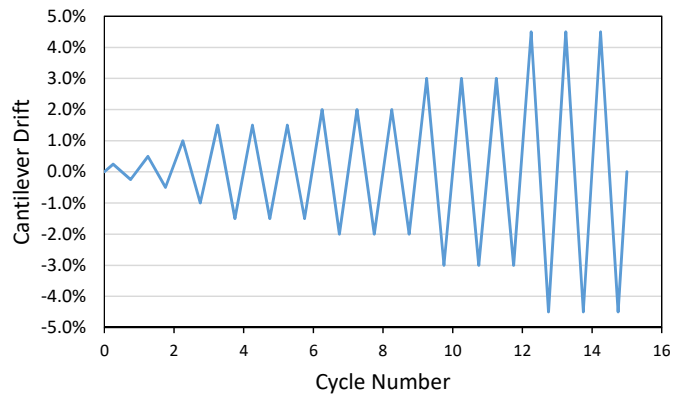
Figure 9: Loading protocol used for cyclic testing

180   **2.4   Instrumentation**

181   In addition to measurement of the applied lateral force and top panel deformation, the

182   panel-foundation connection joint was instrumented with several displacement transducers.   The

183   panels were tested in two phases and so two different instrumentation schemes exist for the panels

184   with 450 mm foundations and those that used either 350 m or 710 mm foundations as is shown

185   Figure 10 and Figure 11 respectively.   For both instrumentation set ups, the opening of the vertical

186   joint at the panel and foundation interface and the potential for vertical cracking to develop in the

15

187   panel were measured at the top, bottom, and mid-height of the foundation. Gauges PG_Top,

188   PG_Mid, PG_Bot measured the gap development between the panel and foundation, and gauges

189   PG_Top CR, PG_Mid CR, and PG_Bot CR measured vertical cracking in the panel for the 450 mm

190   tall foundation specimens (Figure 10c,d). Gauges PG_Top, PG_Mid, and PG_Bot measured both

191   the gap development between panel and foundation as well as vertical panel cracking for the

192   350 mm and 710 mm foundation specimens (Figure 11c,d). Gauge PG_Crack provided an

193   independent crack width measurement for the 350 mm and 710 mm foundation specimens (Figure

194   11d). Horizontal displacement just above and below the panel was also measured (gauges

195   LVDT_Top and LVDT_Bot in 450 mm tall foundations and PG_Gap A and B for the 350 mm and

196   710 mm foundation specimens). The potential for panel uplift and additional rotation about the

197   10 mm thick shims that supported the panel during construction was measured using gauges

198   PG VB_A and B 350 mm and 710 mm foundation specimens, and the panel curvature was

199   estimated using the gauges with the prefix PG V1 or PG V2 for the 450 mm tall foundation

200   specimens. Finally, strain gauges were mounted on the starter bars 20 mm into the foundation.

201
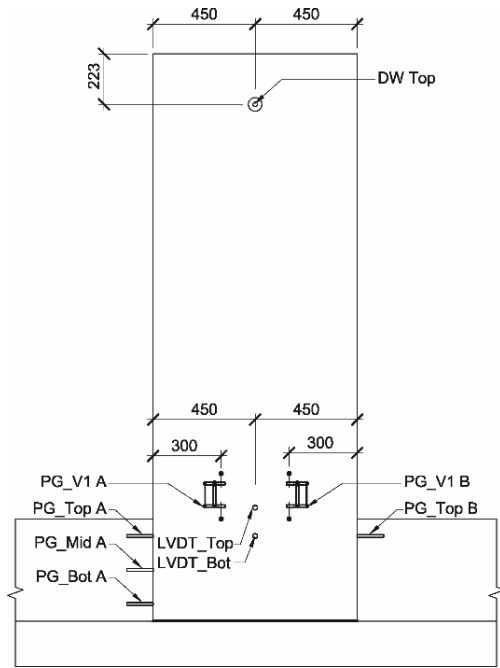
(a) Panel Front
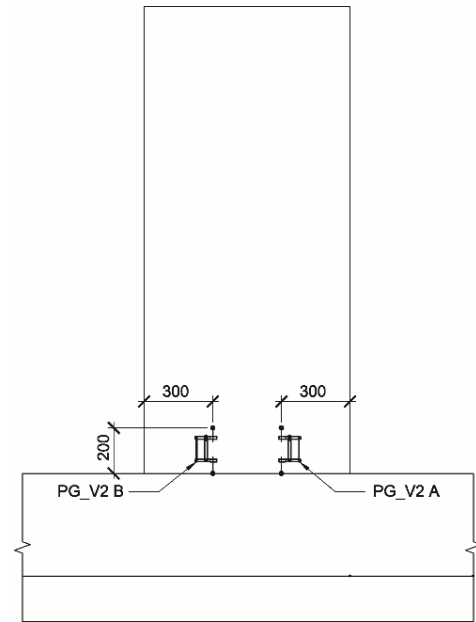
(b) Foundation Face
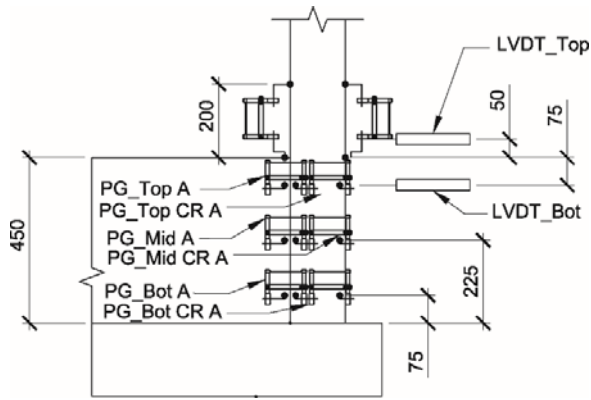
(c) Panel Side A Foundation Instruments
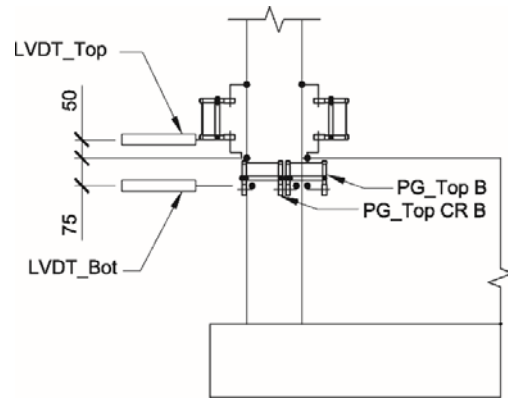
(d) Panel Side B Foundation Instruments

Figure 10: Instrument layout for panels with 450 mm tall foundations. All dimensions in mm, "PG" refers to portal gauge extensometers.
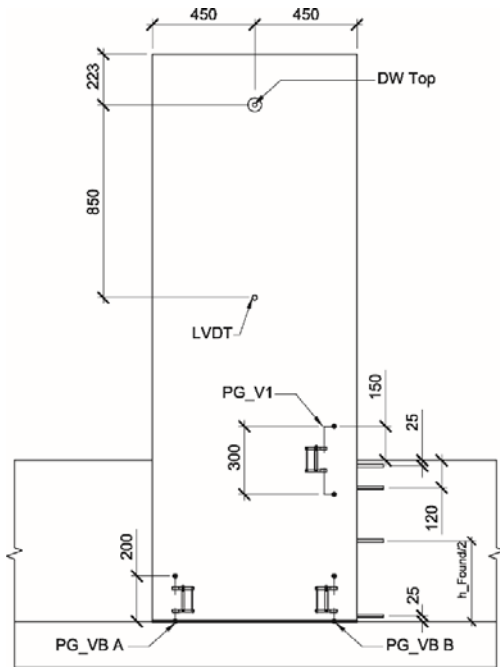
202

(a) Panel Front
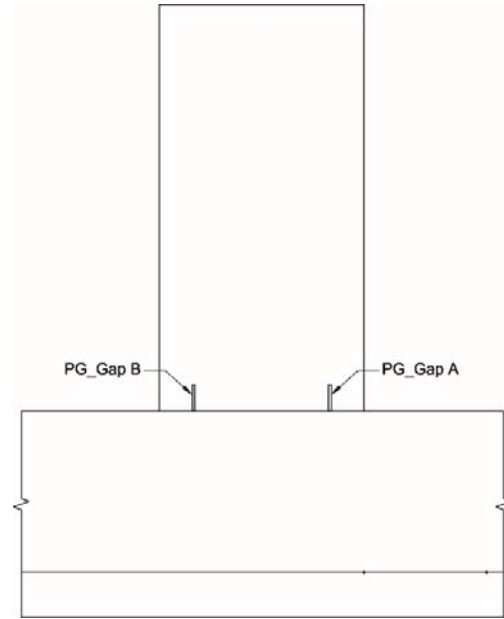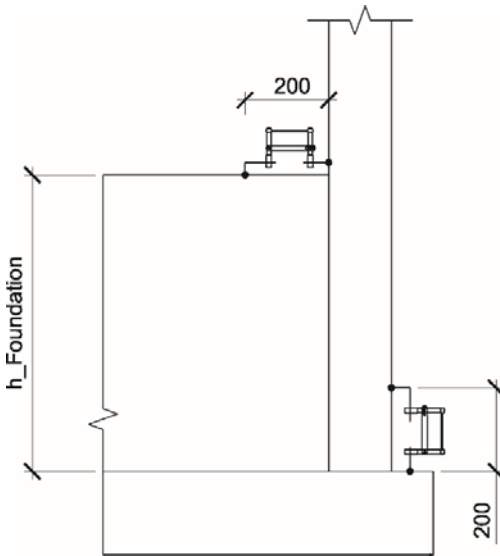
(b) Foundation Face

(c) Panel Side A Foundation Instruments
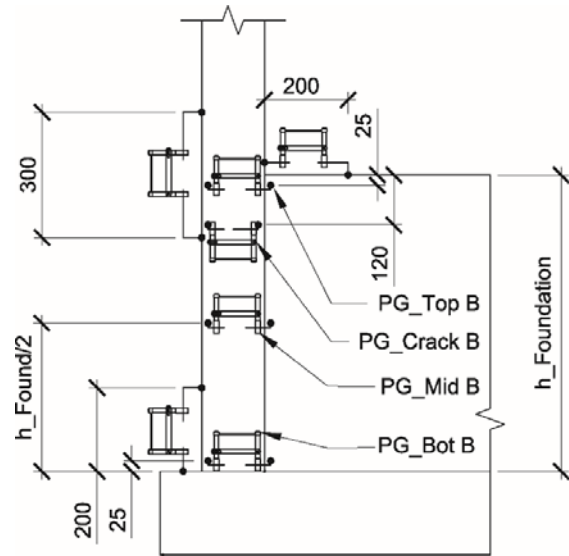
(d) Panel Side B Foundation Instruments

Figure 11: Instrument layout for panels with either 350 mm or 710 mm tall foundations. All dimensions in mm, "PG" refers to portal gauge extensometers.

203

3   TEST RESULTS

204

205   As the panels represented the bottom 2.5 m of a 10 m panel, global behavior of the panels is

206   presented in terms of moment-rotation to characterize the connection behavior. The moment is

207   that is applied to the panel at the top level of the foundation, and the rotation is the calculated from

208   the inverse tangent of the lateral deformation at the applied load divided by the distance from the

209   load to the top level of the foundation. While alternative methods of determining the applied

210   moment and rotation on the connections could be considered due to the influence of the joint on the

211   out-of-plane behavior, the above method was chosen to allow for consistent comparison between

212   panels and directions of loading and is also consistent with the demands that would be estimated by

213   the design engineer. Rotation of the panel to foundation connection joint was determined from the

214   inverse tangent of the displacement at foundation level over the distance to the calculated center of

215   rotation of the joint. The center of rotation was calculated from the relative displacements

216   measured from transducers on the foundation connection.

217   **3.1   Bolted Connection: Control Specimen**

218   Panel BLT12-C0 was tested to benchmark the cyclic panel behavior by providing a clear load path

219   that was consistent with the strut and tie load path described in Figure 2. Panel cracking initiated

220   at 0.5% drift at the foundation level in both joint-opening and joint-closing direction with a

221   corresponding cracking moment of 13.5 kN-m and an initial lateral stiffness of 2.85 kN/mm.

222   Three additional flexural cracks formed at approximately 150 mm intervals above the initial crack

223   at the foundation level, as can be seen in Figure 12.   These additional cracks formed during both

224   the 1% and 1.5% drift cycles.   Crack opening concentrated at the foundation level with the

225   foundation level cracks opening to a width of 4 mm at 4.5% drift.   From the global

226   moment-rotation hysteretic plot shown in Figure 13, it can be seen that the panel reached nominal

227   moment capacity in both the joint-opening and joint-closing directions with strength increases

228   observed until the panel reached 3% drift with an 18 kN-m capacity in the joint-opening direction

229   and a 25 kN-m capacity in the joint-closing direction.   Above 3% drift the strength capacity in

230   each respective loading direction remained constant until the final cycle at 6.5% drift.   No

231   degradation was of strength was observed between different drift levels and the test was ended at

232   6.5% drift due to limitations of jack stroke.   No cracking was observed in the joint (Figure 12),

233   which was consistent with the expectations that the detail provide a clear load path based upon the

234   strut-and-tie model in Figure 2.

235   Significant pinching in the hysteretic behavior was observed, particularly in drift levels above 2.0%

236   (Figure 13).   This pinching resulted from inelastic extension of the single layer of reinforcement

237   coupled with low axial load which meant that the reinforcement did not yield in compression and so

238   flexural cracks could not close until the panel translated through a rotation that was greater than the

239   previous cycle.   Panel BLT12-C0 also displayed a significant amount of asymmetry in the

240 hysteretic response (Figure 13). The panel exhibiting a lower strength and stiffness in the when

241 subjected to joint-opening moments, with the panel not reaching nominal moment capacity in the

242 joint-opening direction until 1.5% drift as opposed to the joint-closing direction in which nominal

243 moment capacity is reached on the first cycle.   Due to the symmetric vertical reinforcing layout,

244 the asymmetric response is a result of the joint geometry and reinforcing.   For joint-closing

245 loading, the panel bears against the top of the foundation and the starter bars are located such that

246 the foundation interface has greater moment capacity than the panel, thus allowing the panel to

247 develop its nominal capacity and subsequent over-strength as expected.   When loaded in the

248 joint-opening direction, the panel-foundation interface cracks, and the panel is loaded with an

249 increased moment arm as it is bearing against a location below the foundation level with the top

250 starter bar in tension.   The additional joint-opening moment is combined with the flexibility of the

251 starter bars deforming in tension to reduce the lateral stiffness in the joint-opening direction.

252 The asymmetric response is also observed in decrease in strength for subsequent cycles at a given

253 drift level.   In the joint-closing direction, there is approximately a 5% drop in strength for

254 subsequent cycles at a given drift level, but in the joint-opening direction the decrease in strength

255 for subsequent cycles at a given drift rotation is as much as 37%.   The significant strength

256 degradation in the joint-opening direction is likely results from concentrated yielding of the starter

257 bars as they deform at the panel-foundation interface and within the oversized PVC duct.

258   A comparison between the measured joint and panel rotations with respect to applied moment at the

259   foundation level is shown in Figure 14.   The joint rotation is calculated by first determining the

260   center of rotation in the joint from the portal gauge sensors on the foundation interface (Figure 10

261   and Figure 11) and calculating the inverse tangent of between the horizontal displacement at the top

262   foundation sensor and the center of rotation.   The horizontal displacement of the panel at the top of

263   the foundation includes both the separation at the panel-foundation interface as well as any potential

264   vertical cracking that could form in the panel joint region.   The panel rotation is calculated by the

265   inverse tangent of the displacement at the applied load minus the displacement of the top foundation

266   sensor divided by the distance from the load to the top level of the foundation.   Most the

267   deformation observed in the test was a result of panel rotation at the large flexural crack at the

268   foundation level, with panel rotation being approximately ten times larger than the joint rotation in

269   the joint-opening direction.   Figure 14 supports that the reduced stiffness in the joint-opening

270   direction resulted from joint deformations as the joint rotations joint-opening direction are

271   approximately seven times larger than those in the joint closing direction.   This discrepancy was

272   expected as in the joint-opening direction the center of rotation occurred between the two layers of

273   starter bars and the moment arm in the joint is between one half and one third of the foundation

274   depth depending on drift level, while in the joint-closing direction, the panel bears against the

275   foundation and the bottom dowels is in tension thus allowing almost the full depth of the foundation

276   to resist the applied moment.

277

(a) Front of panel from Side A   (b) Side B joint behavior

Figure 12: Damage of Panel BLT12-C0 at -4.5% Drift

278
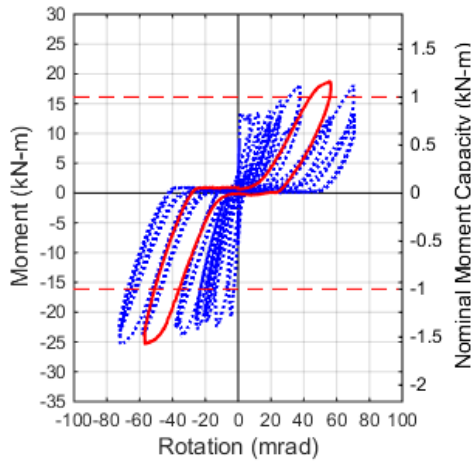
Figure 13: Global Moment-Rotation behavior of Panel BLT12-C0 with 4.5% drift cycle highlighted. Positive values of moment and
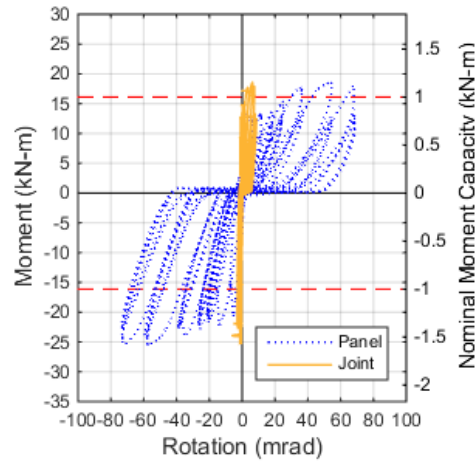
Figure 14: Comparison between rotation in panel and rotation in joint of Panel BLT12-C0

rotation correspond to joint-opening behavior.

279

280 **3.2   Behavior of Details using Conventional Starter Bars**

281 The damage state following cyclic testing of the two panels that utilized conventional starter bar

282 details, Panels DL12-C50 and U12-C50, is shown in Figure 15.   For the panel that utilized two

283 rows of 600 mm 90-degree hooks, Panel DL12-C50, cracking initiated at 0.5% drift in the

284 joint-opening direction at the foundation level.   In the joint-closing direction, four flexural cracks

285 formed starting at the foundation level and at 150 mm increments at 0.5% drift.   The panel had an

286 initial stiffness of 3.4 kN/mm and cracking was a result of 13.8 kN-m at the foundation level.   The

287 crack at 600 mm above foundation had largest opening with a crack width of 2 mm at 2% (Figure

288 15).   The large opening of this crack is due to its location directly above the returns of the hooked

289 bar returns that formed the starter bars (Figure 6a), as these bars effectively tripled the vertical

290 reinforcement ratio and strength below this crack.   At 6.5% drift, crack opening was concentrated

291 just above the hook returns at 600 mm above the foundation in both the joint-opening and

292 joint-closing directions.   An opening of 8 mm was observed at this crack location, and in the

293 joint-opening location a 1.8 mm separation at the panel-to-foundation joint represented the other

294 significant deformation that was observed at this drift level.   Except for the separation between the

295 panel and the foundation, no damage was observed in the joint.

296 The overall moment-rotation response of Panel DL12-C50 is shown in Figure 16.   The panel was

24

297   able to achieve nominal moment capacity in both directions and exceeded nominal moment

298   capacity in the joint-opening direction after 3% drift level and in the joint-closing direction at 0.5%

299   drift.   The panel reached a maximum strength of 21.3 kN-m in the joint-opening direction at 4.5%

300   drift after which the strength degraded to 18.5 kN-m at 6.5%.   In the joint-closing direction, the

301   panel showed an increase in moment capacity until a maximum of -33.8 kN-m was reached at 6.5%

302   drift.   The increased capacity in the joint-closing direction is a result of the returns from the starter

303   bars being offset from the vertical reinforcing and away from the foundation (Figure 6a), which

304   resulted in an deeper effective section in the joint-closing direction.   The panel exhibited similar

305   pinched hysteretic behavior to that which was observed in the BLT12-C0 panel due to the

306   elongation of the reinforcing requiring rotations in excess of the previous cycle before the flexural

307   cracks would close. Cyclic testing was completed at 6.5% drift due to reaching the jack stoke limit.

308   No damage was observed in the joint region, but significant crack widths were noted in the panel.

309   The comparison between joint and panel rotation with respect to applied moment at the foundation

310   level is shown in Figure 17.   No significant joint rotation in the joint-closing direction occurred in

311   Panel DL12-C50 with a magnitude of less than 1 mrad.   In the joint-opening direction a maximum

312   of 8 mrad rotation occurred in the joint, which is a similar amount of joint deformation in the

313   joint-opening direction as the control specimen (BLT12-C0). The small amount of joint-deformation

314   in the joint-closing direction results from the additional reinforcing from the hooks in the joint

315   region forcing deformations to concentrate higher in the panel

316   Panel U12-C50 maintained similar strength and stiffness in both joint-opening and joint-closing

317   directions without significant damage to the joint (Figure 15).   The panel had an initial stiffness of

318   3.2 kN/mm and cracking initiated at foundation level at 0.5% drift in joint-opening direction when

319   subjected to a 19.6 kN-m moment.   At 1.0% drift, an additional flexural crack opened

320   approximately 150 mm above the foundation level on both sides of the panel.   These were the only

321   two cracks to open on the panel face during the test and opened to a maximum 4 mm at the

322   foundation and 6 mm at upper crack in both the joint-opening and joint-closing direction at 4.5%

323   drift.   Vertical cracking was observed on panel sides but remained narrow in the joint region and

324   did not appear to signify the onset of breakout at the joint.   Instead these vertical cracks appeared

325   to result from prying action on the vertical reinforcement and the lack of shear reinforcement in the

326   out-of-plane direction of the panel.

327   Panel U12-C50 exceeded the nominal moment capacity of the panel at 0.5% drift level in both

328   directions (Figure 16).   The panel appeared to reach yield at this drift level as the strength

329   remained constant at approximately -18 kN-m for each drift level in the joint-closing direction.   In

330   the joint-opening direction, the panel increased in strength from 19.6 kN-m at 0.5% and 1.0% drift

331   levels up to 25.4 kN-m at 4.5% drift.   The discrepancy in strengths between the two directions

332   aligns with what would be expected if the vertical reinforcing was offset from center by 10 mm,

26

333   which would be possible if the 75 mm tall reinforcing chairs were oriented 90° prior to casting.

334   No significant reduction in strength was observed between drift levels and the test was completed

335   due to stroke limitations on the loading jack.   Slight spalling at the cracks was observed at the later

336   cycles and it is expected that panel would have failed in a flexural failure rather than joint failure

337   due to the large deformations in the flexural cracks.

338   Panel U12-C50 also had similar joint rotations to the idealized BLT12-C0 connection (Figure 17).

339   The better than expected performance of Panel U12-C50 likely results from efficient transfer

340   between the vertical reinforcement and the starter bars.   Because the starter bars were of Panel

341   U12-C50 were tied directly to the vertical reinforcement and well anchored, the panel was able to

342   more effectively transfer loads between the panel and the foundation than threaded insert panels

343   with similar cover depth behind the starter bars as discussed in the next section.
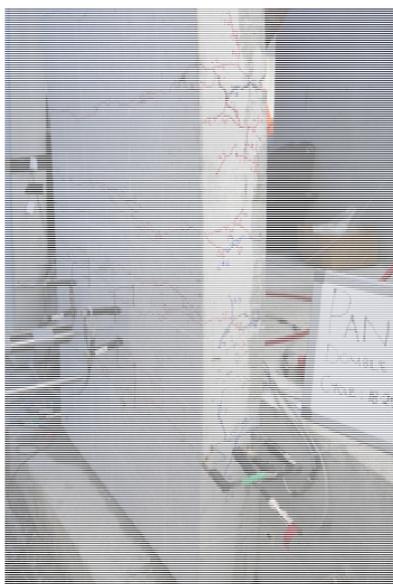
DL12-C50   U12-C50

Figure 15: Damage to specimens with conventional 12 mm starter bars at maximum joint-opening drift

DL12-C50   U12-C50
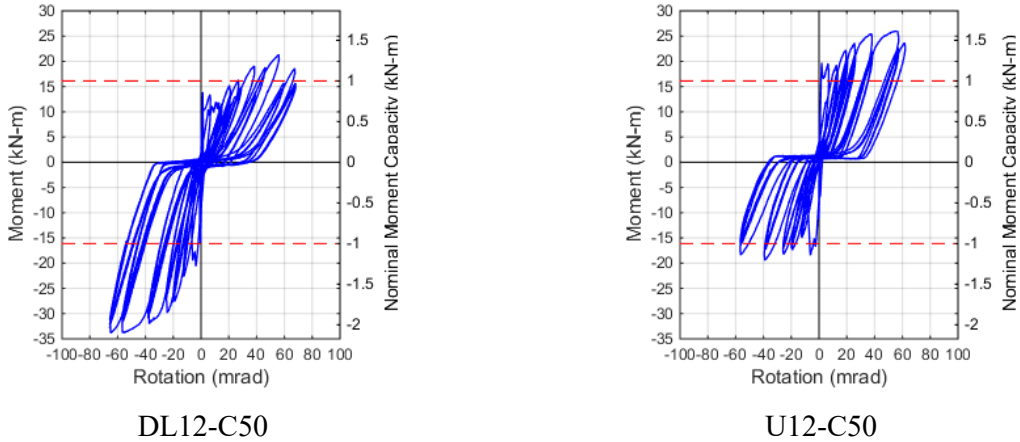
Figure 16: Global moment-rotation behavior of panels with conventional 12 mm starter bars. Positive values of moment and rotation correspond to joint-opening behavior.

DL12-C50   U12-C50
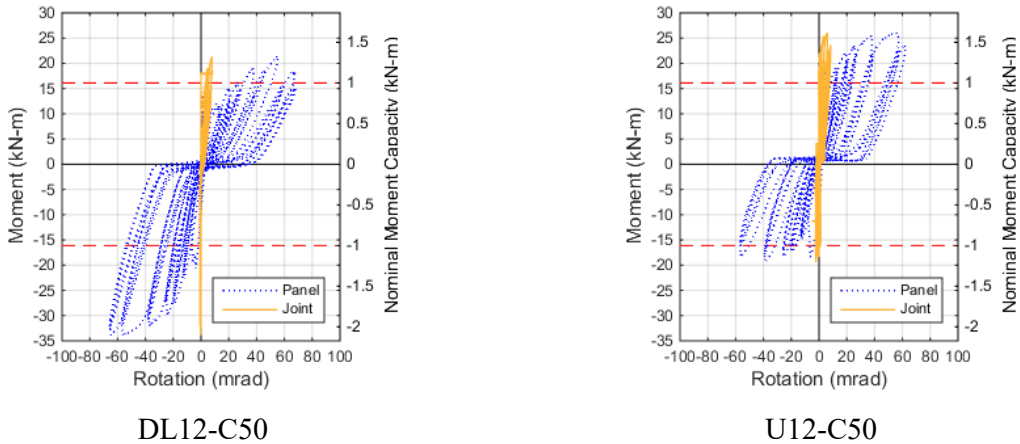
Figure 17: Joint vs panel moment-rotation behavior of panels with conventional 12 mm starter bars. Positive values of moment and rotation correspond to joint-opening behavior.

3.3   Behavior of Details using Threaded Inserts

3.3.1   12 mm Starter Bars

Three panel details utilizing 12 mm threaded inserts were tested and included Panels TI12-C50, TI12-C42, and TI12-C50-FC.   The observed damage of these panels at the end of cyclic testing is shown in Figure 18 while the observed damage to the panel joint following demolition and removal of the panel is shown in Figure 19. The global moment-rotation hysteretic behavior is shown in Figure 20 and the joint rotations and crack widths forming on the side of the panels due to concrete breakout behind the inserts are provided in Figure 21 and Figure 22 respectively.   It should be noted that the calculated joint rotation includes deformation arising from both separation between the panel and foundation as well as any vertical cracking in the panel in the joint region.

| TI12-C50 | TI12-C42 | TI12-C50-FC |
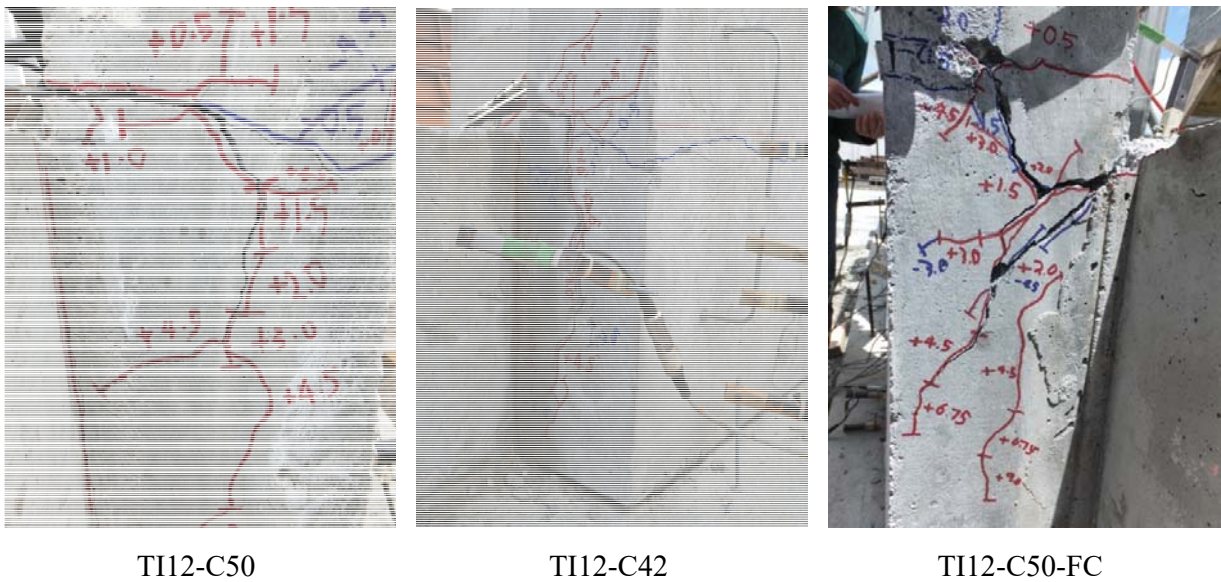
Figure 18: Damage to specimens with 12 mm starter bars at maximum joint-opening drift

| TI12-C50 | TI12-C42 | TI12-C50-FC |

Figure 19: Observed joint damage to 12 mm insert panels following panel demolition

358
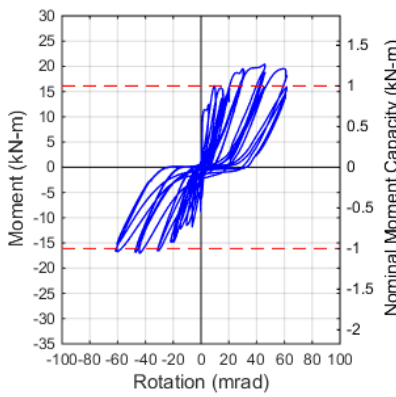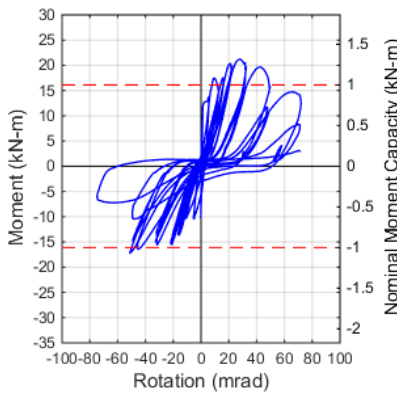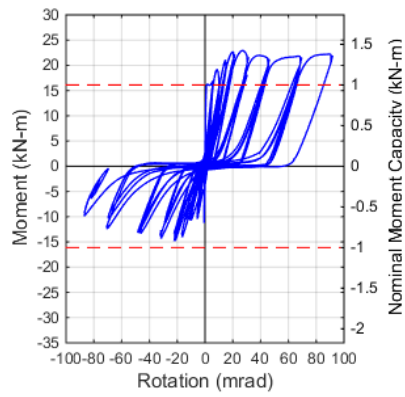
| TI12-C50 | TI12-C42 | TI12-C50-FC |

Figure 20: Global moment-rotation behavior of panels with 12 mm starter bars and inserts. Positive values of moment and rotation correspond to joint-opening behavior.

359
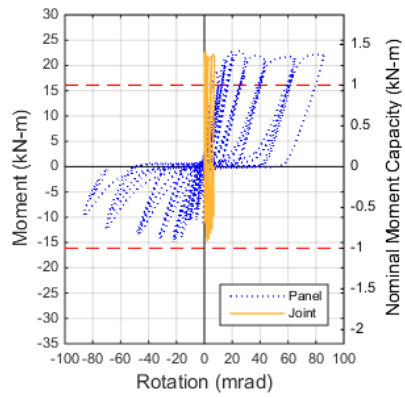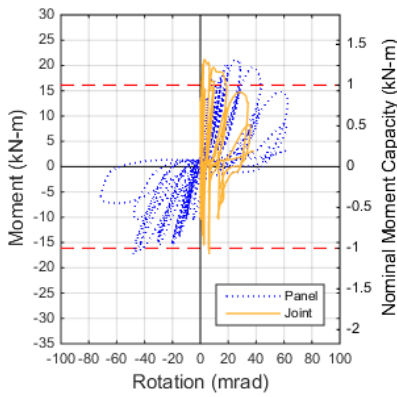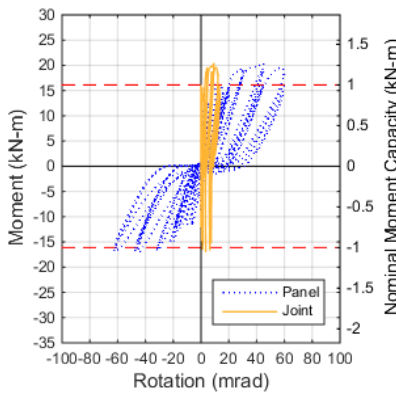
Figure 21: Joint vs panel moment-rotation behavior of panels with 12 mm starter bars and inserts. Positive values of moment and rotation correspond to joint-opening behavior.

360

TI12-C50   TI12-C42   TI12-C50-FC
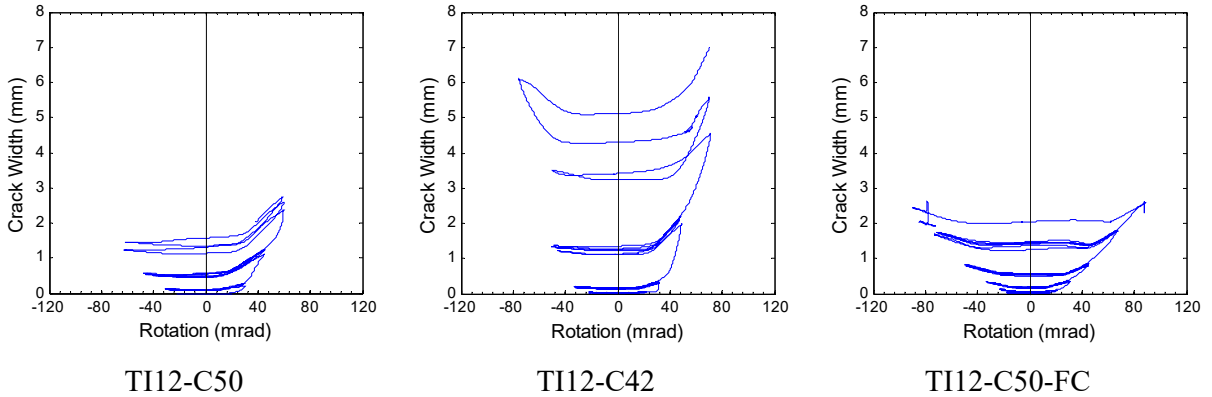
Figure 22: Typical width of vertical crack forming behind threaded insert with respect to panel rotation for panels with 12 mm starter bars

361   3.3.1.1 **Panel TI12-C50**

362   Panel TI12-C50 utilized two rows of three inserts which were installed flush to the panel-foundation

363   interface with an embedment depth of 100 mm (Figure 7a).   The panel had an initial stiffness of

364   1.4 kN/mm and cracking initiated in the panel just above foundation level at 0.5% drift when

365   subjected to an 11.4 kN-m moment.   An additional flexural crack formed approximately 300 mm

366   above foundation at 1% drift, and the crack at foundation level began to extend vertically towards

367   the base of the panel.   At 1.5% drift, an additional flexural crack at 150 mm above foundation, and

368   the vertical crack in joint began to extend down to the level of the top dowels, and by 3% drift the

369   vertical crack in the joint had extended down to 120 mm below foundation level with a width of

370   0.6 mm at the top end.   At 4.5% drift, the panel vertical cracking continued to extend to three

371   quarters the depth of the foundation and curved around back towards the foundation, similar to a

372   cone breakout crack pattern (Figure 18).   At 6% drift, the vertical crack extended to within 25 mm

373   of the base of the panel, and post-test demolition of the panel revealed that a breakout-style failure

374   plane had formed behind the top level of inserts (Figure 19).

375   Overall the panel had experienced a stable hysteretic response, but with significant pinching.   The

376   specimen reached the nominal moment capacity of the panel at 2% drift, and by 3% drift the panel

377   had reached its maximum strength of 20.4 kN-m in the joint-opening direction and 17 kN-m in the

378   joint-closing direction (Figure 20).   Most of the deformation occurred in the panel, but

379   joint-opening rotations were a maximum of 14 mrad which is about 1.7 times larger than the

380   corresponding joint-opening rotations in Panel U12-C50, mostly due to the addition of vertical

381   cracking in the panel joint region.   Joint-closing rotations were similar to those in the joint-opening

382   direction because the vertical crack behind the inserts remained open even when subjected to

383   joint-closing moment, as can be seen in Figure 22.

384   3.3.1.2 **Panel TI12-C42**

385   Panel TI12-C42 utilized an 8 mm thick nail plate to install the inserts, which was removed prior to

386   casting the foundation.   As such the end of the insert where the starter bar was threaded in was not

387   located at the panel-foundation interface.   Similarly to Panel TI12-C50, Panel TI12-C42 had an

388 initial stiffness of 2.1 kN/mm and experienced initial cracking at the foundation level at 0.5% drift

389 when subjected to a 13 kN-m moment.   At 1% drift, a second flexural crack formed 200 mm above

390 the foundation, and vertical cracking in the panel joint initiated from the flexural crack at the

391 foundation level and extend to 50 mm below the foundation level.   By 2% drift, this vertical crack

392 had extended to 100 mm below the foundation level, but was still of less than 0.5 mm limited width.

393 At 3% drift no new cracks had formed and the deformation concentrated at the foundation level.

394 The vertical crack extended to over half the depth of the foundation and opened up to a similar

395 width as the flexural crack in the panel where it initiated.   Cracking was observed over the entire

396 height of the panel-foundation interface and resulted from both joint-opening and joint-closing

397 actions.   At 4.5% drift the vertical crack in the joint extended to within 25 mm of the bottom of the

398 panel and has opened up to over 2 mm (Figure 18).   As can be seen from post-demolition

399 inspection in Figure 19, a breakout-style failure plane formed behind all of the inserts in a similar

400 manner to that which was observed in Panel TI12-C50.

401 The panel exhibited hysteretic behavior similar to the other panels at low drifts.   In the

402 joint-opening direction, the panel reached capacity at 2.0% drift with a moment capacity of

403 21.1 kN-m, after which the peak response degraded to 8.3 kN-m during the second cycle of the

404 4.5% drift level.   In the joint-closing direction, the panel increased strength with each cycle until it

405 reached an ultimate capacity of -17 kN-m at -3.0% drift, which was only just slightly over the

406   nominal moment capacity of the panel. The panel moment capacity dropped in the following

407   cycle due to the damage sustained to the joint in the joint-opening direction. This joint damage

408   resulted in significant joint rotations of up to 35 mrad, which was almost three times as large as that

409   observed in Panel TI12-C50 (Figure 21) and equal to approximately half of the rotation that

410   occurred due to the panel deformations. These large joint rotations were a result of the vertical

411   crack in the joint which opened up to 6 mm wide (Figure 22). As with the other tested specimens,

412   significant hysteretic pinching was observed due to elongation of the single layer of reinforcing,

413   which may have been exacerbated by the low joint stiffness and vertical cracking of the panel in the

414   joint region.

415   The addition of the nail plate appears to have caused the panel to perform worse than if it were

416   neglected. When no nail plate was used and the insert was at the panel-foundation interface, such

417   as on Panel TI12-C50, there was a larger crack opening the panel and foundation interface than

418   when for Panel TI12-C42 which utilized a nail plate. This additional interface opening likely

419   resulted in slip of the threaded bar in the insert, which Ma (2000) noted was an average of 0.28 mm

420   for this type of threaded insert. This additional flexibility would have reduced the joint-opening

421   rotational demand on the panel demand for a given the same level of drift as can be seen in the

422   hysteretic response in Figure 20 and would have resulted in less breakout behind the inserts (Figure

423   19).

3.3.1.3 Panel TI12-C50-FC

Panel TI12-C50-FC had threaded inserts installed in a similar method as Panel TI12-C50, except

they were spaced both horizontally and vertically such that the theoretical failure cones of adjacent

inserts did not intersect. To accommodate this spacing, the panel was connected to a 710 mm deep

foundation. The panel had an initial stiffness of 5.6 kN/mm and cracking initiated at the

foundation level at 0.5% drift. At 1% drift an additional flexural crack opened at approximately

200 mm above foundation and a vertical crack extended from the foundation level flexural crack

into the panel joint. An additional crack at panel-foundation interface formed during joint-opening

which extended downwards at approximately 30° towards the joint on one of the panel edges.

Vertical cracking at mid-depth of panel was observed extending from both flexural cracks in both

upwards and downwards direction. These cracks appear to result from prying of the vertical

reinforcement and lack of shear reinforcement in the out-of-plane direction rather than due breakout

of the joint. At 2% drift, the vertical crack in the joint extended to 75 mm below foundation, and

the interface crack which extended downwards towards the joint at 45° appeared on the opposite

panel end. This angled crack extended to a depth of approximately 120 mm below the foundation

and ended at mid-depth of the panel. This crack also extended to the foundation, resulting in a

small amount of spalling, and suggested that the dowel was deforming at the interface. At the 2%

drift level the panel reached a maximum strength of 22.6 kN in the joint-opening direction. The

442   panel was able to maintain a similar strength in the joint-opening direction out to 6.5% drift, but

443   with a significantly pinched hysteresis.   The panel also reached a maximum joint-closing strength

444   of -14.6 kN at 2% drift, which was below the nominal moment capacity of the panel.   A steady

445   strength degradation was observed in the joint-closing direction between the 3.0% and 6.5% drift

446   levels.   By 4.5% drift, the vertical crack extended to approximately 200 mm below foundation,

447   which was the location of the top row of dowels, and the joint crack angled at 45° opened to

448   4.0 mm in the joint-opening direction.   In the joint-closing direction, the flexural crack at the

449   foundation level opened on the tension face to a width of 8.0 mm and the flexural crack on the

450   compression side did not fully close, which would explain the reduction in apparent strength in this

451   direction.   The vertical crack in the joint remained open and the panel appeared to "kick out" at the

452   foundation level.   Post-demolition investigation did not reveal any break out behind dowels

453   (Figure 19), and crushing of the compression zone started to occur at 6.5% drift.

454   As shown in Figure 21, Panel TI12-C50-FC exhibited a similar magnitude of joint rotation in the

455   joint-opening directions as observed in Panel DL12-C50, even though a crack width of up to

456   2.5 mm was measured (Figure 22).   It is expected that this limited rotation was observed because

457   the foundation was twice as tall as the other 12 mm insert connections and the location of the insert

458   205 mm below the foundation line (Figure 7e) meant that the vertical crack in the panel only just

459   reached the level of the top row of starter bars and as such the panel connection still was able to

460   maintain fixity with the top row of starter bars.

461   **3.3.2   12 mm Starter Bar Monotonic Tests**

462   Several monotonic tests were also performed on panels to investigate the joint-opening behavior of

463   the panels directly, or in the case of Panel DL12-C50, a monotonic push to failure using as steel

464   packer to increase the tested displacement after cyclic loading.   Figure 23 and Figure 24 show that

465   the panels with threaded insert connections behaved similarly when subjected to either cyclic or

466   monotonic loading, with a vertical crack propagating behind the inserts of the panels with a 350 mm

467   tall foundation and relatively little damage occurring in the joint of the panels with a 710 mm tall

468   foundation.   The change in failure mechanism for the different foundation heights suggests that the

469   failure mechanism described in Figure 2 is dependent upon the relative strength between the panel

470   and foundation connection.

471   Panel DL12-C50, which during cyclic loading had damage concentrated at the point where the

472   starter bar hooks terminated, failed during monotonic loading by splitting of the panel at the depth

473   of the vertical reinforcement (Figure 23).   This failure was brittle when compared to the panels

474   with inserts as can be seen from the relative rotations of the joint and panel in Figure 21 and Figure

475   25.   During monotonic loading the panel lost strength rapidly after a rotation of 110 mrad and

476   significant joint rotations were detected as the vertical crack propagated behind the vertical

477   reinforcement.   Conversely, Panel TI12-C42 experienced large joint rotations as a result of vertical

478   cracking behind the inserts, but lost strength in a more controlled manner.

TI12-C42-M   TI12-C50-FC-M   DL12-C50
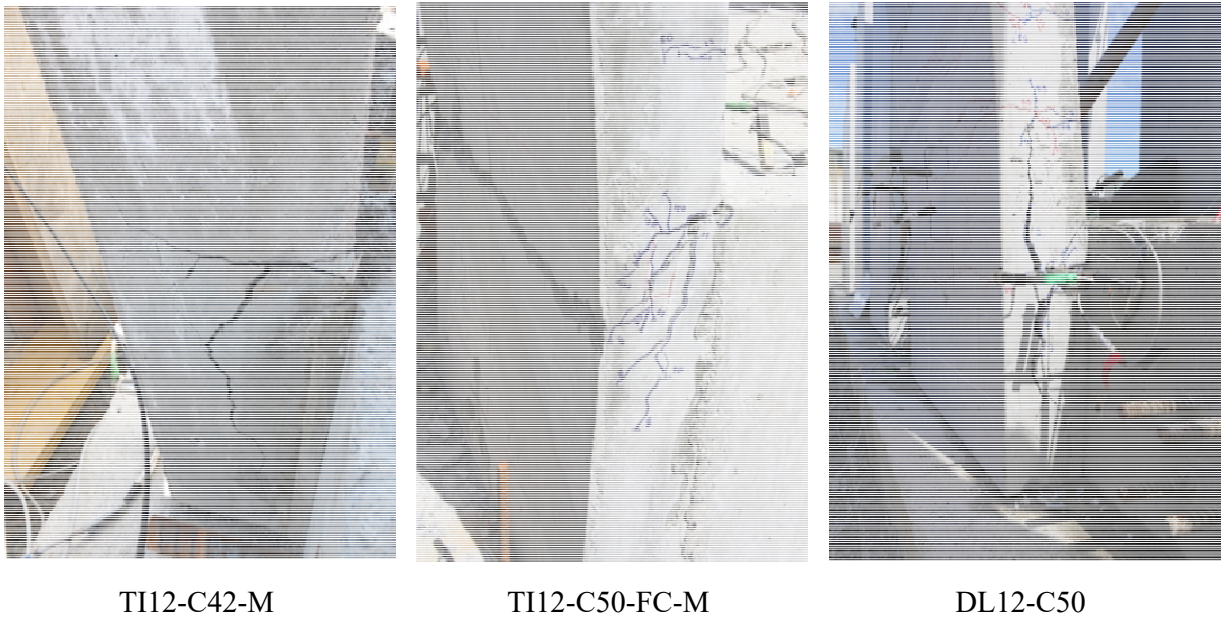
Figure 23: Damage to specimens with 12 mm starter bars following monotonic pushover in joint-opening direction

479
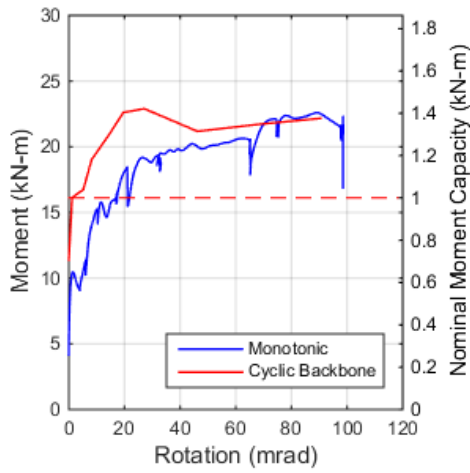
Figure 24: Comparison between cyclic backbone and monotonic joint-opening moment-rotation behavior of TI12-C50-FC-M.
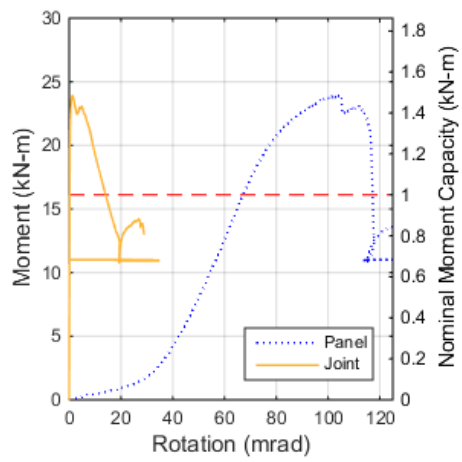
Figure 25: Joint vs panel joint-opening moment-rotation behavior of Panel DL12-C50.

38

3.3.3   Behavior of Details using 16 mm Starter Bars

Three panel details utilizing 16 mm threaded inserts were tested and included Panels TI16-C32,

TI16-C24, and TI16-C50-FC.   These details were tested both cyclically and monotonically, with

the specimens that were tested monotonically denoted with an "M".   The observed damage of

these panels at the end of cyclic testing is shown in Figure 26 while the observed damage to the

panel joint following panel demolition is shown in Figure 27. The global moment-rotation

hysteretic behavior is shown in Figure 28 and the joint rotations and crack widths forming behind

the inserts are provided in Figure 29 and Figure 30 respectively.   It should be noted that the

calculated joint rotation includes deformation arising from both separation between the panel and

foundation as well as any vertical cracking in the panel in the joint region.
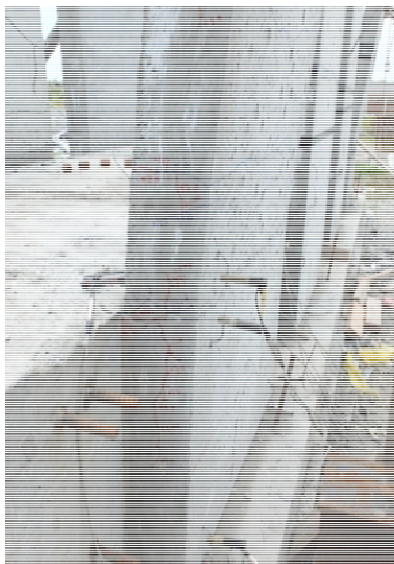
| TI16-C32 | TI16-C24 | TI16-C32-FC |
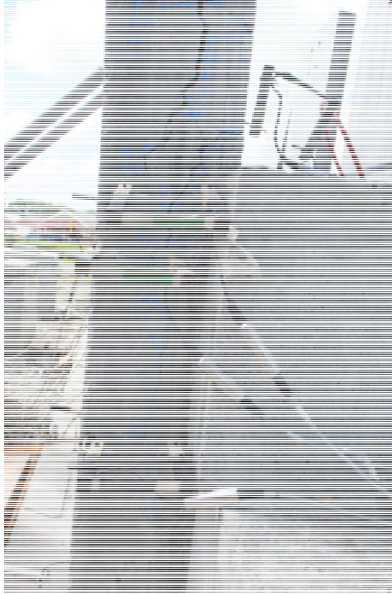
TI16-C32-M   TI16-C24-M   TI16-C32-FC-M

Figure 26: Damage to specimens with 16 mm starter bars at maximum joint-opening drift

490

TI16-C32   TI16-C24   TI16-C32-FC

TI16-C32-M   TI16-C24-M   TI16-C32-FC-M

Figure 27: Observed joint damage to 16 mm insert panels following panel demolition

491
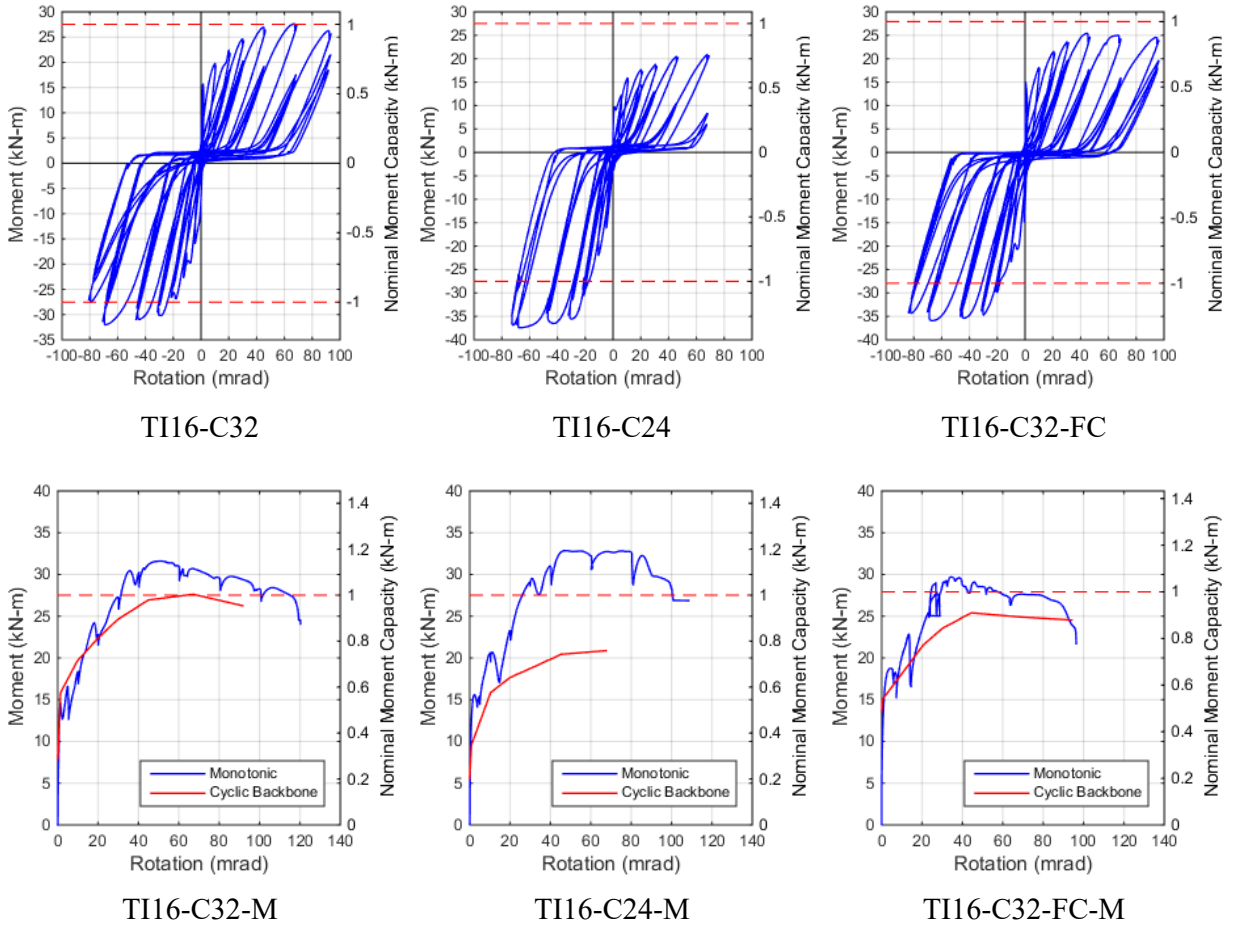
Figure 28: Global moment-rotation behavior of panels with 16 mm starter bars and inserts. Positive values of moment and rotation correspond to joint-opening behavior.

492
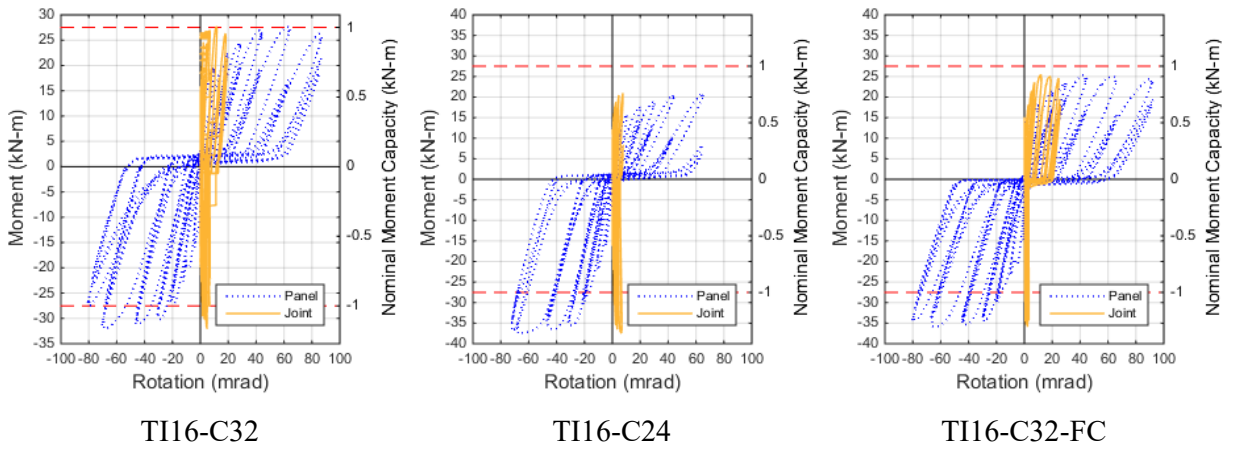
Figure 29: Joint vs panel moment-rotation behavior of panels with 16 mm starter bars and inserts. Positive values of moment and rotation correspond to joint-opening behavior.

493

| TI16-C32 | TI16-C24 | TI16-C32-FC |

| TI16-C32-M | TI16-C24-M | TI16-C32-FC-M |
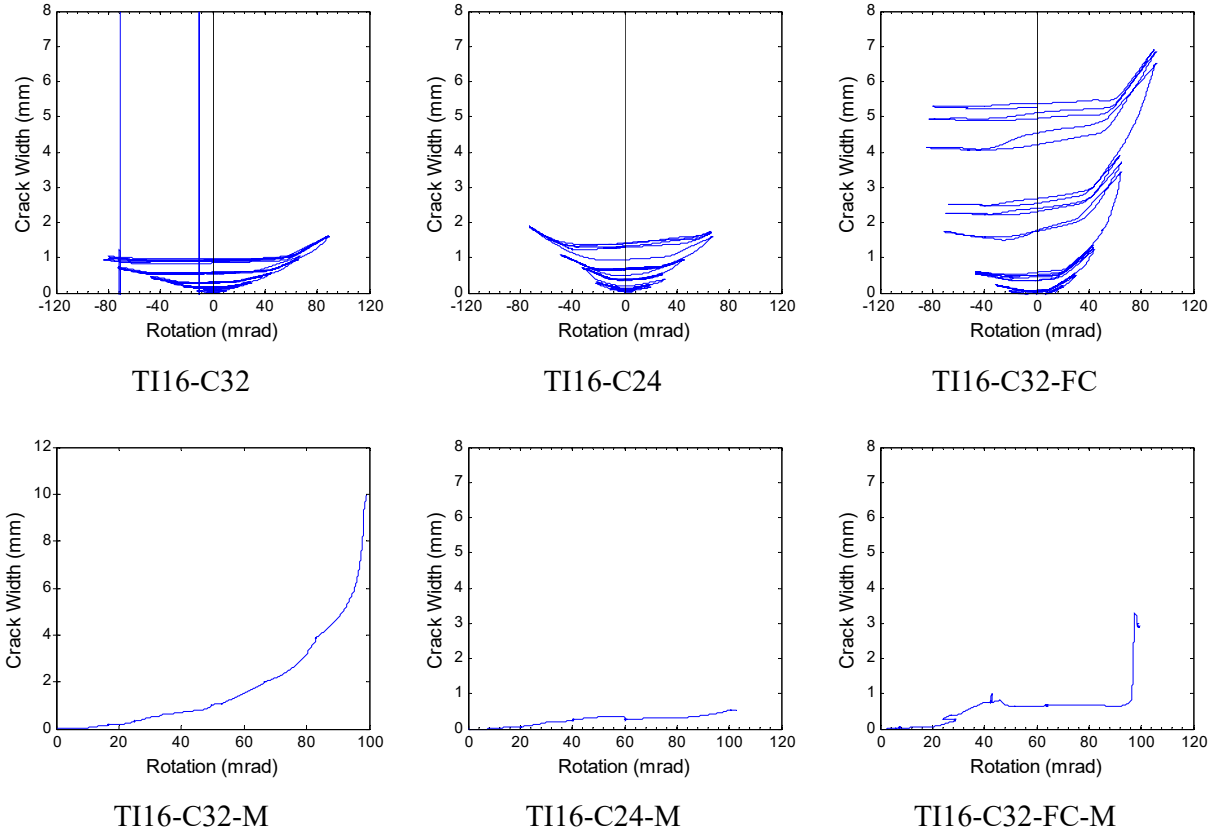
Figure 30: Typical width of vertical crack forming behind threaded insert with respect to panel rotation for panels with 16 mm starter bars

494   3.3.3.1   **Panel TI16-C32**

495   Panel TI16-C32 was constructed with threaded inserts installed flush to the panel-foundation

496   interface with and embedment depth of 118 mm (Figure 8a). The panel had an initial stiffness of

497   4.4 kN/mm with cracking just above the foundation level occurring at 15.8 kN-m. At 1% drift in

498   the joint-opening direction, a vertical crack propagated from the foundation level flexural crack at

499 mid-depth of the panel and extended to 100 mm below the foundation level. An additional

500 flexural crack opened when loaded in the joint-closing direction approximately 280 mm above the

501 foundation height. During the 2% drift cycle, the vertical crack in the joint extended to 150 mm

502 below foundation and a third flexural crack formed at 500 mm above foundation. The panel

503 exceeded its nominal moment capacity in the joint-opening direction at 3.0% drift with a maximum

504 strength of 26.9 kN-m that was sustained in subsequent joint-opening drift levels. Vertical

505 cracking formed at the mid-depth of the panel at the other flexural cracks and extended both in the

506 upwards and downwards direction by 50 mm to 75 mm. In the joint-closing direction the panel

507 reached nominal capacity at 3% drift and increased in strength to -32 kN at 4.5% drift until strength

508 degradation occurred during the 6.75% cycle to a joint-closing capacity of -27.5 kN. By the 4.5%

509 drift level, the vertical crack in the joint extended 225 mm below the foundation level and was

510 2.0 mm wide at the flexural crack and 1 mm wide at 120 mm below the foundation level (Figure 30),

511 and at 6.75% drift vertical crack in the joint extended to 250 mm below foundation causing a joint

512 rotation of 20 mrad (Figure 29). Following post-test demolition, it was apparent that breakout had

513 occurred behind two of the three threaded inserts (Figure 27).

514 The monotonically loaded panel, Panel TI16-C32-M, exhibited similar crack propagation as the

515 cyclically loaded panel, but showed a 20% increase in observed strength when compared to the

516 cyclically loaded specimen TI16-C32 (Figure 28). The crack propagation in TI16-C32-M also

517   included the extension of vertical cracks at mid-depth of the panel from each flexural crack, except

518   there was a greater opening of the vertical crack between the foundation level flexural crack and the

519   flexural crack that occurred 200 mm above the foundation line (Figure 26). At 6% drift, the

520   vertical crack at panel mid-depth between the first two flexural cracks connected, and at 8% drift

521   had opened to at least 2.0 mm (Figure 30). Also at 8% drift cracking in the joint extended to at

522   least half of the foundation depth (350 mm), and finally at 10% drift one longitudinal bar fractured

523   and the vertical cracks in the joint opened substantially and connection to all of the inserts was lost

524   (Figure 27).

525   3.3.3.2 **Panel TI16-C24**

526   Panel TI16-C24 was constructed with an 8 mm nail plate that was removed prior to casting of the

527   foundation (Figure 8b). During cyclic loading, the panel exhibited an initial stiffness of

528   4.2 kN/mm with cracking at foundation level occurring at 0.5% drift when subjected to a moment of

529   9.6 kN-m. At 1% drift, vertical cracking extended from the foundation level crack in both the

530   upwards and downwards directions at the mid-depth of the panel, and at 2% drift, an additional

531   flexural crack formed at approximately 200 mm above the foundation, which also had small vertical

532   cracks extending at mid-depth. By 3% drift, three more flexural cracks had opened at 150 mm

533   intervals up the panel. In the joint-opening direction, the vertical crack in the joint extend to

534   approximately 150 mm below the foundation level and in the joint closing direction and an

535   additional crack in the joint formed from the foundation level to the mid-depth vertical crack with a

536   downwards inclination such that the two cracks intersected at 100 mm below the foundation line.

537   The foundation level flexural crack opened to a width of only 1.6 mm and the vertical cracks in the

538   joint remained less than 1 mm wide.   At 4.5% drift, foundation flexural crack extended to 200 mm

539   below foundation line but only of moderate width (Figure 26).   Relatively little rotation was

540   observed in the joint (Figure 29) especially given the similar crack width were observed in the joint

541   when compared to Panel TI16-C32 (Figure 30)

542   Panel TI16-C32 experienced a maximum joint-opening strength of 20.8 kN-m, which was only

543   about 75% of the nominal moment capacity of the panel.   In joint-closing direction, panel achieved

544   a 37.4 kN-m capacity, which was similar to that observed in the other 16 mm insert connections

545   (Figure 28).   Cyclic damage to the threads of the inserts, as has been identified previously by Ma

546   (2000), or improper installation of the starter bars is the most likely cause for the low joint-opening

547   strengths observed in Panel TI16-C24, especially since the vertical crack width was relatively small

548   compared to Panel TI16-C32-FC (Figure 30) suggesting that significant breakout did not occur

549   behind the insert heads.   Additionally, there was a larger panel-foundation interface opening in

550   Panel TI16-C24 than in the monotonically loaded panel with the same reinforcement, TI16-C24-M,

551   and the monotonically loaded panel also exhibited much greater strength and deformation capacity

552   (Figure 28) suggesting slip of the starter bar in the insert.

553   During monotonic loading, cracks initiated at foundation and at 1% drift extended into the joint and

554   at the panel-foundation interface. Vertical cracking extended upwards from flexural crack at

555   mid-depth of the panel, as was observed in the other 16 mm insert panels.   By 4% drift two more

556   flexural cracks had opened up at 200 mm intervals above the foundation.   Both cracks had vertical

557   cracks extending from the ends of the cracks including one that extended from the flexural crack

558   200 mm above the foundation to end approximately 15 mm from the compression face of the panel.

559   At 6% drift, the crack 200 mm above the foundation opened to over 5 mm, the vertical crack near

560   the compression face extended to 150 mm above the foundation, and joint cracking extended to

561   mid-depth of foundation.   Finally, when the panel reached 10% drift, a large vertical crack

562   formed at mid-depth of the panel that connected the flexural cracks at the foundation level and the

563   one 200 mm above this level.   Limited cracking occurred in the joint during the monotonic test had

564   due to the large crack opening 200 mm above the foundation.   Both cyclic and monotonic tests

565   showed signs of breakout between behind the top row of inserts (Figure 27), but substantial damage

566   observed of splitting of panel at mid-depth just above the foundation during the monotonic test.

567   3.3.3.3 **Panel TI16-C32-FC**

568   Panel TI16-C32-FC was constructed with the inserts flush to the panel-foundation interface, but

569   spaced such that a full theoretical failure cone could form (Figure 8d, e).   Initial cracks formed at

570   the foundation level, with vertical cracking extending up and down at mid-depth when subjected to

571   a 15.0 kN-m moment.   By 2% drift, additional flexural cracks had formed 200 mm and 400 mm

572   above the foundation both with vertical cracking extending to 50 mm above and below the flexural

573   cracks at mid-depth of panel.   During cycles to 2% drift the vertical joint crack had extended down

574   to 150 mm below foundation level.   During the 3% drift joint-closing excursion a crack formed in

575   the joint from the foundation level at the panel-foundation interface and extended down to the

576   vertical joint crack 100 mm below the foundation level, in a similar manner as was observed in

577   Panel TI16-32C.   At 3%, the panel reached its maximum capacity in both the joint-opening and

578   joint-closing directions.   The maximum -35 kN-m capacity in the joint-closing direction was

579   maintained for all subsequent excursions in the joint-closing direction.   The panel was not able to

580   achieve nominal moment capacity in the joint-opening direction with a maximum moment capacity

581   of only 25 kN-m, which was also maintained at subsequent drift levels (Figure 28).   At 4.5% drift

582   the vertical crack in the joint reached down to 200 mm below the foundation level with large crack

583   at panel-foundation interface and 5 mm crack width, and at 6.75% the vertical crack extended to

584   half foundation depth (Figure 26).   Over 20 mrad rotation occurred in the joint (Figure 29),

585   resulting mostly due to the large crack opening in the joint, as can be seen in Figure 30, and lead to

586   breakout behind two of the three inserts in the top row of starter bars (Figure 27).

587   The monotonic test exhibited similar crack propagation as the cyclic test, with initial flexural

588   cracking occurring at foundation level and extending vertically into the joint.   As drift increased, a

589   crack formed at the panel-foundation interface and a second horizontal crack formed approximately

590   150 mm below foundation line, just above the top row of inserts.   Deformation was then

591   concentrated in the panel-foundation interface, the horizontal crack 150 mm below the foundation,

592   and the vertical crack in the joint from the location of the top layer of inserts downwards.   As such,

593   the vertical crack where the side portal gauge was located remained less than 2 mm (Figure 30) as

594   deformation was concentrated at the panel-foundation interface at this level. The monotonic test

595   reached a maximum strength of 30 kN-m, but this capacity degraded after 40 mrad rotation to

596   22 kN-m at 90 mrad as the panel separated behind the inserts, and post-test demolition confirmed

597   that breakout had occurred behind all the inserts.

598   **4   KEY OBSERVATIONS**

599   **4.1   Panel Behavior in Buildings**

600   Most of the tested panels reached nominal flexural capacity in both directions, with only two of the

601   cyclically loaded panels (TI16-C24 and TI16-C50-FC) below nominal capacity in the joint-opening

602   direction and only one panel (TI12-C50-FC) below nominal capacity in the joint-closing direction.

603   However, many panels only just exceeded the nominal capacity and were unable to develop

604   significant flexural over-strength.   In addition, all panels demonstrated a severely pinched

605   hysteretic behavior which resulted from the low axial load and inelastic extension of the single layer

606   of reinforcing requiring large rotations in the panel before the flexural cracks closed.   This failure

607   to close flexural cracks meant that the panel was effectively pinned at the base as it rotated through

608   drift angles below the previous peak rotation.   This change in base fixity has potential implications

609   on the boundary conditions of these panels assumed during design.   If these panels were designed

610   assuming base fixity, and the panel base exhibits the pinched behavior shown in the test specimens,

611   the panel will behave like a simply supported member, shifting bending demands from the more

612   heavily reinforced panel base to the mid-height of panel during out-of-plane face loading.   This

613   behavior is consistent with observations following the Canterbury earthquake sequence in which

614   flexural cracks were observed at the mid-height of some precast panels (Henry and Ingham 2011).

615   A simplified elastic analysis was performed to investigate the level of drift demand required to

616   develop the nominal capacity at the base of the panel, which would create an effectively pinned

617   based due to the highly pinched hysteretic behavior of these panels.   Ignoring panel inertial

618   loading, the lateral roof displacement required to initiate the nominal moment capacity of the 10 m

619   tall fixed-cantilever prototype in this study (see Figure 3) was calculated with equation 1.

$$M_{drift} = \frac{3EI\delta}{h^2} \qquad\qquad \text{[EQ 1]}$$

620   Where M_{drift} is the moment at the base of the panel due to lateral displacement at the top of the

621   panel, E is the modulus of elasticity of the concrete, I is the moment of inertia of the section, δ is the

622   lateral displacement at the panel top, and h is the height of the panel.

623   The drift required to initiate cracking of the panel was calculated using gross section properties of

624   the panel and was assessed for two different cracking moments, the first being determined using the

625   concrete modulus of rupture from NZSEE 3101:2006 (Standards New Zealand 2006) resulting in a

626   cracking moment of M_{cr} = 12.8 kN-m (lower-characteristic strength) and the second cracking

627   moment determined from the test results and was equal to M_{cr} = 15 kN-m. The additional drift

628   that was required to develop the nominal flexural capacity of the panel was computed using cracked

629   transformed section properties of the panels.

630   The additional base moment demand resulting from inertial face loads on the panel was determined

631   using equation 2:

$$M_{inertia} = \frac{wh^2}{8}$$
[EQ 2]

632   Where $M_{inertia}$ is the moment at the base of the panel due to inertial loading, and w is the uniformly

633   distributed load of the panel unit mass multiplied by lateral acceleration. The effect of inertial

634   loading was accounted for by calculating the reduced drift demand to initiate cracking of the panel.

635   The effects of dynamic amplification of panel inertial loads were not accounted for in this

636   simplified analysis.

637   Using Eqns. 1 and 2, the roof drifts required to develop the flexural strength of the 10 m tall

638   prototype panel with either HD12 or HD16 reinforcing is summarized in Table 2. The drifts

639   required to develop the HD12 reinforced panels range from 1.4% drift to 3.8% drift while the drifts

640   to develop the HD16 panels are significantly larger and range from 8.1% to 9.8%. It should be

641   noted that these value only indicate the drifts required to develop the nominal flexural strength of

642   the panel and do not incorporate the behavior of the joint. The drift required to develop panel

643   strength in Table 2 is highly dependent on the assumed cracking moment of the panel. This

644   sensitivity to assumed cracking moment is due to the location of the single layer of reinforcing at

645   mid-depth of the panel which results in a cracked section stiffness approximately twenty times more

646   flexible than the gross section. For the HD12 panels, which are near the minimum reinforcement

647   ratio, the drift required to develop the nominal flexural capacity of the panel is relatively small since

648   the nominal moment capacity of the panels (M_n = 16.1 kN-m) is only slightly higher than the

649   cracking moment. The large drifts required to develop the HD16 panels is a result of the nominal

650   capacity of the panels (M_n = 27.5 kN-m) being almost twice the cracking moment and as such,

651   large displacements would be required to generate the nominal moment demand with the cracked

652   and flexible panels.

653

Table 2: Lateral drift required to develop nominal strength 10 m tall prototype panel in out-of-plane direction

Panel Reinf.	M_{cr} = 12.8 kN-m Acc = 0 g	M_{cr} = 15 kN-m Acc = 0 g	M_{cr} = 12.8 kN-m Acc = 0.1 g	M_{cr} = 12.8 kN-m Acc = 0.2 g	M_{cr} = 15 kN-m Acc = 0.1 g	M_{cr} = 15 kN-m Acc = 0.2 g
HD12	3.8%	1.8%	3.6%	3.5%	1.6%	1.4%
HD16	9.8%	8.5%	9.6%	9.4%	8.3%	8.1%

654

655   Given that lengths of the buildings that utilize these panels commonly exceed 50 m long and have

656   flexible roof diaphragms, the drifts required to develop the HD12 panels (1.4% to 3.8%) are likely

657   to be exceeded during seismic loading.   Once the nominal moment is exceeded, a drift of 2%

658   would cause sufficient rotation demand to cause breakout of the joint and degrade the lateral

659   capacity of the panel.   This preliminary analysis highlights the need to perform a more extensive

660   study to determine the demands on these panels when accounting for diaphragm movement, inertial

661   face loading, and the restraint stiffness at the top of the panel.

662   **4.2   Comparisons to Past Tests**

663   Similar cyclic testing of precast panel-to-foundation connections was performed by Ma (2000).   A

664   total of four panels were tested, with panels that were 150 mm thick, 900 mm wide, and 1400 m tall

665   with a RB12 mm reinforcing and starter bars.   Two of the panels utilized threaded inserts with a

666   130 mm embedment depths at the panel-to-foundation connection, and the other two panels utilized

667   hooked starter bars with 180 mm long returns bent up into the panel.

668   In general the connection details tested by Ma preformed worse than those discussed in this testing

669   program, with none of the Ma panels able to achieve the panel nominal flexural capacity in the

670   joint-opening direction.   Both hooked bar inserts panels exhibited significant strength degradation

671   following the first cycle in the joint-opening direction where after approximately 20 mrad of joint

672   rotation breakout of the hooked bars occurred.   The poor performance of these hooked bar

673   specimens is in contrast to the performance of Panel DL12-C50 in which no damage occurred in the

674   joint.   Such discrepancy can be related to the difference in return length of the hooked starter bars,

675   with short 180 mm returns used for the Ma tests compared to the 600 mm used in Panel DL12-C50.

676   The longer starter bars in DL12-C50 over-reinforced the joint, forcing damage and hinging further

677   up in the panel, and limiting the rotational demand at the foundation level on the starter bars.

678   The 12 mm threaded inserts tested by Ma had a 130 mm length, resulting in a 15% deeper

679   embedment in the 150 mm thick panels when compared to those presented in this paper, which are

680   representative of current construction practice.   Unit 1 of the Ma study had five RB12 vertical

681   reinforcing bars, and during testing the joint exhibited an inclined crack that extended downward

682   into the joint from the foundation level flexural crack.   Post-test demolition investigation revealed

683   evidence of a cone breakout type failure plane.   Unit 4 of the Ma test had only three RB 12 vertical

684   reinforcing bars and during testing only experienced cracking at the panel-foundation interface with

685   no evidence of cone breakout behind the inserts.   The discrepancy in the joint-behavior of these

686   two panels as well as the lack of joint failure in Panel TI12-C50-FC suggests that the failure mode

687   is dependent on the relative strengths of the panel and the foundation connection.   However, the

688   inserts breakout failure mode is non-ductile relying on the concrete tensile capacity and is not

689   considered a desirable load-path.

690   **4.3   Influence of Relative Panel and Joint Strength**

691   In order to investigate the relationship between the panel to joint strength ratio and breakout behind

692   the threaded inserts, the joint strengths (Mcb) of the threaded insert panels in this and the Ma (2000)

693   study were calculated based upon the equations for anchorage pull out that are provided in both ACI

694   318-08 Appendix D (ACI 2008) and NZSEE 3101:2006 (Standards New Zealand 2006). This

695   calculation represents current practice for the design of these connections. For panels in which

696   inserts were spaced such that group action was in effect, the load was applied at the top row and the

697   eccentricity between the anchor group centroid and load was accounted for. An alternative

698   breakout strength was also calculated in which only the top row of inserts was assumed to be

699   effective and assuming that the area of the failure cone was cut-off at the foundation level flexural

700   crack (Mcb*). No strength reduction factors were applied to the calculated panel or joint strengths.

701   The calculated joint strengths were compared to the nominal flexural capacity of the panel section

702   and are summarized for all panels in Table 3.

703   The calculated joint capacities did not predict the breakout of any of the panels except for Panel

704   Ma-1. For all other panels, the calculated joint strength was at least 1.4 times larger than the panel

705   nominal flexural capacity. For the panels with 16 mm inserts, all of which exhibited breakout

706   behind the inserts, the calculated joint strengths were a minimum of 2.9 times larger than the

707   nominal flexural capacity of the panels. While the calculated strengths did not provide accurate

708   representation of the breakout joint failure mode that was observed in the test panels, the large joint

709   to panel strength ratio of 7.6 in the TI12-C50-FC panels does qualitatively support the lack of

710 breakout of the joint for this test.

711 The discrepancy in performance between the calculated joint strength and the observed test

712 behavior suggests that the use of these anchorage equations is inappropriate for the design of such

713 panel details.   This inappropriateness was attributed to these equations being intended for the

714 design of anchors or anchor groups in direct tension instead of the predicting the interaction

715 between the propagation of a flexural crack and the brittle failure of anchor pullout.   Alternative

716 design methods are required to more accurately estimate the strength and failure mode of the

717 panel-to-foundation joints with dowel type connections.

Table 3: Comparison of panel and connection strength of threaded insert panels

Panel Name	Connection Description	Vert Reinf	Mn Panel (kN-m)	Mcb Joint (kN-m)	Mcb/Mn	Mcb* Joint[d] (kN-m)	Mcb*/Mn	Breakout Observed
TI12-C50	TI12	HD12	16.1	20.0	1.2	25.2	1.4	yes
TI12-C42	TI12 + Nail plate	HD12	16.1	20.0	1.2	25.2	1.4	yes
TI12-C42-M	TI12 + Nail plate	HD12	16.1	20.0	1.2	25.2	1.4	yes
TI12-C50-FC	TI12 Full Cone	HD12	16.1	123.2	7.6	120.1	7.4	no
TI12-C50-FC-M	TI12 Full Cone	HD12	16.1	123.2	7.6	120.1	7.4	no
TI16-C32	TI16	HD16	27.5	169.5	6.2	79.7	2.9	yes
TI16-C32-M	TI16	HD16	27.5	169.5	6.2	79.7	2.9	yes
TI16-C24	TI16 + Nail plate	HD16	27.5	169.5	6.2	79.7	2.9	yes
TI16-C24-M	TI16 + Nail plate	HD16	27.5	169.5	6.2	79.7	2.9	yes
TI16-C32-FC	TI16 Full Cone	HD16	27.9	154.7	5.5	123.8	4.4	yes
TI16-C32-FC-M	TI16 Full Cone	HD16	27.9	154.7	5.5	123.8	4.4	yes
Ma-1	TI12	HD12	19.9	17.5	0.9	17.9	0.9	yes
Ma-4	TI12	HD12	12.3	17.5	1.4	17.9	1.5	no

[a] TI = Threaded Insert; number following is diameter of starter bar

[b] M in panel name denotes monotonic loading

[c] All vertical reinforcing spaced at 270 mm

flexural crack

718   5   CONCLUSIONS & FUTURE WORK

719   Fourteen precast panel connections were subjected to out of plane loading to assess the out-of-plane

720   seismic performance of dowel type precast panels.   The panel connections represented typical

721   dowel type connections used in the precast industry and included both threaded inserts and

722   conventional starter bars.   The following key observations and conclusions were made from the

723   tests:

724   • All but two of the panels that utilized threaded insert connections experienced vertical

725   cracking in the joint and breakout of behind the insert head confirming the brittle load path

726   in this connection.   These panels mostly exceeded the nominal moment capacity of the

727   panel in the joint-opening direction, but degraded in strength and stiffness after 20 mrad of

728   rotation.

729   • The conventional starter bar details limited damage to the panel with the joint remaining

730   undamaged by strengthening the panel at the foundation level or as was the case with the U

731   bar connection, but efficient transfer of load between the vertical reinforcing and the

732   foundation.

733   • All panels experienced significantly pinched hysteretic response as a result of plastic strains

734   in the single layer of reinforcing and low axial load causing axial elongation, with large

735   rotations required to close flexural cracks in the panels.

736   • The assumption of the panels acting as fixed cantilevers in the out-of-plane direction likely

737   to be inappropriate for panels with vertical reinforcement content close to the minimum

738   reinforcement ratio as the drifts required to develop the nominal flexural strength of the

739   panel are likely to be reached in the flexible diaphragm buildings that utilized these panels.

740   Once nominal panel strength is reached in these panels, the panel base is effectively pinned

741   due to the low axial load and inefficient crack closure of these panels, and the maximum

742   flexural demand would shift to mid-height of the panel during face-loading.

743   • It was found that the use of anchors pullout design equations does not predict the

744   performance of these threaded insert connections because these design equations were not

745   intended to account for combined actions, including the propagation of flexural cracking

746   behind the insert head.

747   Due to the poor performance but prevalent use of threaded insert connections, an additional study

748   was performed to develop connection details that utilized threaded inserts but avoided the loss of

749   load path behind the insert head.   This study is detailed in a companion paper entitled:

750   *Out-of-Plane Behavior of Foundation Inserts of Precast Panels: Existing Connections.*

6 REFERENCES

ACI (2007). Acceptance Criteria for Special Unbonded Post-Tensioned Precast Structural Walls Based on Validation Testing and Commentary. ACI ITG-5.1M-07. Farmington Hills, MI, American Concrete Institute.

ACI (2008). Building code requirements for structural concrete (ACI 318-08) and commentary. Building code and commentary. Farmington Hills, Mich., Farmington Hills, Mich. : American Concrete Institute 2008.

ACI (2013). Guide for testing reinforced concrete structural elements under slowly applied simulated seismic loads. ACI 374.2R-13. Farmington Hills, MI, Farmington Hills, MI : American Concrete Institute 2013.

Adham, S., H. Tabatabi, H. Brooks, L. Brugger, G. Dick, A. Hamad, J. Kariotis, D. Nghim, R. Phillips, A. Salama, C. Sramek, J. Stanton, S. Wood, L. Cluff and B. Lizundia (1996). "TILT‐UP‐WALL BUILDINGS." Earthquake Spectra **12**(S1): 99-123.

Beattie, G. (2007). Design Guide: Slender Precast Concrete Panels with Low Axial Load. Judgeford, New Zealand, Building Research Association of New Zealand (BRANZ)**:** 65.

Hamburger, R. O., D. L. McCormick and S. Hom (1988). "Whittier Narrows, California earthquake of October 1, 1987-performance of tilt-up buildings." Earthquake Spectra **4**(2): 219-254.

Henry, R. and J. Ingham (2011). "Behaviour of tilt-up precast concrete buildings during the 2010/2011 Christchurch earthquakes." Structural Concrete **12**(4): 234-240.

Ma, M. (2000). Methods of joining precast concrete components to form structural walls Master's Thesis, University of Auckland.

Seifi, P., R. S. Henry and J. M. Ingham (2016). "Panel Connection Details in Existing New Zealand Precast Concrete Buildings." Bulletin of the New Zealand Society for Earthquake Engineering **49**(2): 190-199.

SESOC (2013). Interim Deisgn Guidance. Design of Conventional Structural Systems following the Canterbury Earthquakes, Structural Engineering Society New Zealand.

Standards New Zealand (2006). NZS 3101:2006. Concrete Structures Standard, Part 1, The Design of Concrete Structures, Standards New Zealand.